“Predicting the mineral composition of dust aerosols. Part 2: Model evaluation and identification of key processes with observations” by Perlwitz et al.

Dear Yves,

As with the companion article, we are grateful for the thoughtful comments of the reviewers and we appreciate the extra time to make substantial revisions in response. Some of the comments have also been used in the companion article to expand the model description or clarify our discussion of the results.
Our response to each of the reviewer comments below contains a reference to a page number or section of the revised article where a change was made. (Where the change is limited to a sentence or two, we also quote the change in our response.) We think these references will make it clear how we have attempted to improve the article in response to the reviewers’ comments.

Best wishes,

Ron Miller
Jan Perlwitz
Carlos Peréz García-Pando

Response to the Comments by Reviewer #1

(The pages and line numbers to which Reviewer #1 refers seem to correspond to the version submitted after the technical review (but before publication in *Atmos. Chem. Phys. Disc.*). We have listed in **bold** the page and line numbers that we believe correspond to the discussion version.)

General comments

This study addresses modeling and validation aspects of dust mineral composition. The subject of the research is crucially important for better understanding the multiple roles of dust in climate system. The authors conduct the analysis using global model with nudged wind fields and exploit the available observations and soil databases. They test two clear hypotheses about the mineral emission fractions. The main problem is that the observational base is relatively poor both for soil parameters database, which uses observations with insufficient spatial resolution, and for aerosol observation that are sporadic in time and space. However, we have to admit that this is the best available information at a time. It is important to start working in this direction. The global approach has advantage, as it allows incorporating available observations all over the world. However, it is low resolution and is very poorly supported by observations in the Southern Hemisphere. Similar regional studies have to be encouraged in future. The minor comments are given below.

Thanks for these supportive remarks. We agree that there are large uncertainties in the data base for the soil mineral fractions, which are used as input for our simulations, and that our evaluation would benefit from a far greater number of measurements. Like Claquin et al. (1999), we accepted these uncertainties because we believe that mineral composition is fundamental to how dust aerosols interact with climate. We hope that our work draws the attention of scientists who do measurements, who can offer improved contraints upon the models.

Minor comments

I would suggest the authors once more report their emission scheme. It would be more convenient for a reader to have this information just in the text but not in the references.'

As suggested by the reviewer, we have added a new section summarizing the dust aerosol module, including the calculation of emission (Sect. 2.2, starting on p. 8).

P 3, 25-30: It sounds like the most important assumptions are semi-hypothetical. Could you elaborate on this and add explanations. **(Page 3580, lines 1-6)**

We have tried to identify more precisely in Sect. 2 (with full details in the companion paper: Perlwitz et al., 2015) where our method depends upon hypotheses or empirical representations suggested by measurements. For example, we note that the allocation of silt emission into the size categories transported by the model is based upon measurements at a single location (as noted below) and we discuss the validity of this representation (p. 6, last paragraph).

P 4, 1-10: Dust particles will be processed in the atmosphere both microphysically and chemically. You have to clearly discuss this and mention what model actually accounts for. **(Page 3580, lines 7-16)**

We do not account for this process in the current version of the model. Following the referee's suggestion, we explicitly note this in Sect. 2.2 (p. 9, penultimate paragraph). We have also added this point to the companion article.

> "These modifications, which depend upon the mineral composition, alter the solubility and vulnerability of the dust particle to wet scavenging. We defer representation of this dependence to a future study and assume the solubility of each dust 25 particle to be constant (50%) and identical for each mineral (Koch et al.,

> 1999).”

P 4, 20: I do not think it is good idea to nudge winds at all levels assuming, e.g., that the surface flow is strongly controlled by the topography and it is different in the GISS ModelE and NCEP reanalysis. I would nudge in the boundary layer. Is nudging coefficient altitude dependent? Please elaborate on this issue. **(Page 3580, line 27)**

The reviewer raises an interesting point. However, the NCEP/NCAR reanalyses toward which we nudge have horizontal resolution of $2.5^\circ \times 2.5^\circ$ latitude by longitude, which is similar to the resolution of ModelE2. In practice, we don't expect that the difference between the topographies should be large. In response to the reviewer, we note in Sect. 2.3 (p. 10) that the nudging time scale is independent of height and equal to 100 s (and we also add this information to the companion article). We would be grateful to be pointed toward any study where nudging of winds only within the boundary layer provides better agreement with measurements.

> “The horizontal winds at each level of the model are relaxed every six hours toward the NCEP reanalyzed values (Kalnay et al., 1996). Relaxation occurs at all model levels (up to 10 hPa) with the globally uniform time scale of 100 s.”

P 4, 25: Aerosol optical depth is the most important observed/retrieved characteristic. There should be some comparison included. **(Page 3581, line 6)**

We agree that this would be a useful exercise. However, in the present version of the model, we do not use the mineral fractions to calculate AOD because this task (along with model evaluation) requires substantial effort, and is deferred to a future study. We note this emission explicitly in the revised manuscript (Sect. 2.2, last paragraph on p. 9).

> “We also defer calculation of radiative forcing as a function of the aerosol mineral composition. As a result, radiative feedbacks between the mineral fractions and

> climate are disabled."

P 5, 3: Change "will be" to "are" **(Page 3581, line 10)**

Done. (Top of Sect. 2.1, p. 5)

> "Two simulations are compared to our compilation of observations."

P 5, 5-10: MMT covers the entire world but how many observations they really had to build those mineralogical fields?' **(Page 3581, lines 12-18)**

The MMT is based on 239 "descriptions of soils", covering dry areas from the United States, Israel, Australia, North Africa, China, Iran, Iraq, and Northern India (Claquin et al., 1999). We are not sure whether "description" refers to soil samples or identifications of individual minerals (or something else), so we have not added this information to the article. Claquin et al. emphasize the uncertainty remaining in the MMT, which motivated subsequent refinements by Nickovic et al. (2012) and Journet et al. (2014).

P 5, 10-15: Is there any physical bases why we can assume that iron oxides are equally abandoned in clay and silt fractions? Could you please clarify this issue. **(Page 3581, lines 18-22)**

There are only limited size-resolved measurements of iron oxides and their fraction in the soil (e.g. Journet et al., 2014). Claquin et al. (1999) infers the soil fraction of iron oxides from color rather than measurements at specific particle sizes, and assumes that iron oxides are present only at silt sizes. However, subsequent aerosol measurements show that iron oxides are present at both clay and silt sizes (Lafon et al., 2006; Kandler et al., 2007; Engelbrecht et al., 2009; Jeong et al., 2014). Consistent with Nickovic et al. (2012), we assume that the iron oxide fraction at clay sizes is identical to MMT value at silt sizes prescribed by Claquin et al. (1999). We are not aware of measurements that would allow a more precise distribution of iron oxides with respect to particle size. We discuss this in Sect. 2.1 at the bottom of p. 5.

> “According to the MMT, hematite is present in the soil only at silt sizes. Aerosol measurements show this mineral to be present at both clay and silt sizes (Lafon et al., 2006; Kandler et al., 2007; Engelbrecht et al., 2009; Jeong et al., 2014), so we extend the size range of emitted hematite to include clay sizes. Given the limited measurements of this mineral in soil samples, we follow Nickovic et al. (2012), and assume for simplicity that the hematite fraction at clay sizes in identical to the silt fraction provided by the MMT.”

P 5, 20-25: Is it observations from one place used to verify the distribution of minerals over the size bins? Please comment on this and clarify in the text. **(Page 3581, line 28 to page 3582, line 5)**

Yes. For the AMF experiment, we use measurements at the single location of Tinfou, Morocco by Kandler et al. (2009) to derive a normalized distribution of mass for each mineral within the silt size category (with diameters between 2 and 50 μm). This distribution is used to apportion the emitted silt fraction into the size categories of ModelE2 at every source region. The distribution is normalized so that it is independent of the specific magnitude of emission at Tinfou. We assume that the (normalized) size distribution is invariant with respect to source region. There are few measurements that would allow us to evaluate this assumption, but we think that the emission increase with particle diameter is probably robust (Sect. 2.1, p. 6, last paragraph).

P 5, 25-26: Please clarify the sentence about “gravitational setting”. **(Page 3582, line 6)**

This is a typo that was intended to say “gravitational settling”, i.e., the falling out of dust particles due to gravity (p. 6, line 13).

> “Dust at Tinfou is measured after transport from the source, when the largest particles are removed preferentially by gravitational settling.”

P 6 10-15: It is not empirically based, it is just an assumption. Could you explain. **(Page 3582, lines 19-24)**

We agree, and now describe our reconstruction as a “heuristic” representation, which we believe is more descriptive than “empirical’. We are expressing the idea that fully dispersive measurements of the soil destroy aggregates that would have persisted during mobilization and brittle fragmentation. Thus, the emitted silt fraction contains silt particles present in the wet-sieved soil, but also aggregates comprised of wet-sieved clay particles. In Kok (2011), the number of aggregates of diameter D scales with the volume fraction of soil particles with sizes below or equal to this diameter. This expression predicts that the fractional contribution of clay soil particles to the emitted silt mass scales with the soil clay fraction. This is the behavior that we are representing heuristically by allowing wet-sieved clay particles to contribute to the emitted silt fraction in proportion to our coefficient γ (Sect 2.1, p. 7).

> “In the AMF simulation, we reaggregate these fragments heuristically. For each mineral, the emitted silt fraction is comprised of silt particles in the wet-sieved soil augmented in pro- portion to the mineral’s wet-sieved clay fraction . . . .”

P 6, 18-21: Please clarify both about the constrain and about transformation of mineral fractions. **(Page 3582, line 18 to page 3583, line 3)**

We deleted the word “transformation”. What we are trying to express is the *contrast* between the SMF and AMF mineral fractions. This contrast results from accounting for aggregates that are potentially emitted from the original soil, but destroyed by wet sieving (Sect 2.1, p. 7).

> “The emitted silt fraction consists not only of silt particles present in the wet-sieved soil, but also aggregates that were broken during wet sieving into clay-sized fragments. In the AMF simulation, we reaggregate these fragments heuristically . . . .”

P 6, 22-25: Please justify this assumption. **(Page 3583, lines 3-5)**

The extension of feldspar and gypsum to the clay-sized range, which are absent in the MMT in this size range, is justified by the fact that these minerals are present at this size in aerosol measurements (Leinen et al., 1994; Arnold et al., 1998; Kandler et al., 2007, 2009). We have added a justification and references for the extension in Sect. 2.1 (p. 7, bottom).

> “Conversely, the MMT provides the fraction of feldspar and gypsum only at silt sizes, even though aerosol measurements show that these minerals are present at both clay and silt sizes (Leinen et al., 1994; Arnold et al., 1998; Kandler et al., 2007, 2009).”

P 7, 14-16: Does this emitted mass in your model produces reasonable dust optical depth? It would be useful to mention this in the text. **(Page 3583, lines 25-28)**

In the current version in the model, we haven’t calculated the scattering and absorption of radiation by the mineral tracers. We agree that the aerosol optical depth should be evaluated. However, this is both beyond the capability of the current model and the scope of the current study. The focus of this study is the evaluation of the model mineral fractions, which is independent of the scaling of the absolute dust mass and the dust aerosol optical depth. Our model emission is within the range calculated by other models, which gives some confidence that the dust AOD in the new model won’t be outside the current range of uncertainty. We intend to calculate the radiative effect and evaluate the model AOT in a future study. In

Sect. 2.2 (p. 9, last paragraph), we note the omission of any radiative perturbation by the minerals.

> “We also defer calculation of radiative forcing as a function of the aerosol mineral composition. As a result, radiative feedbacks between the mineral fractions and climate are disabled.”

P 9, 6-25: XRD and SEM have a disadvantage to be more sensitive to the particle surface layer that could be affected by coating. **(Page 3585, line 21 to page 3586, line 12)**

Thanks. We have added this caveat (p. 12, line 23).

> “Both XRD and SEM measurements are disproportionately sensitive to composition on the particle surface, which may include coatings resulting from chemical reactions with other species, compared to the particle interior.”

P 14, 21-25: Isn’t it directly follow from our assumptions for the SMF and AMF emissions? **(Page 3591, lines 15-19)**

The result discussed by the reviewer is the overestimate of the quartz fraction at silt sizes by the SMF method, with improved agreement within the AMF experiment (p. 18, around line 15 of the current draft). The reviewer seems to be asking whether this improvement is inevitable. We believe that this is not the case.

The smaller quartz fraction in the AMF experiment compared to the SMF simulation indeed follows directly from accounting for reaggregation in the former (that increases phyllosilicate emission at silt sizes at the expense of the quartz fraction). However, it is *not* inevitable that the AMF value is closer to the observed value. For example, the MMT could have indicated a quartz fraction at silt sizes in the SMF experiment that is consistent with the observed value. Then, reaggregation within the AMF simulation would still decrease the quartz fraction, but move it *away* from the measurements. The fact that the SMF value is an underestimate shows that accounting for phyllosilicate reaggregation is necessary. That the combination of the MMT and reaggregation of phyllosilicates (i.e. the AMF method) results in approximately the observed value suggests that the MMT quartz fraction is approximately correct.

P 15, 15-17: It would be useful to take more about how atmosphere could process dust particles. **(Page 3592, lines 9-12)**

We have expanded the discussion in Sect. 2.2 about physical and chemical transformation of dust particles during transport and our current neglect of these processes (p. 9, penultimate paragraph).

> “Measurements show that physical and chemical properties of aerosols evolve along their trajectory (cf. Baker et al., 2014). . . . These modifications, which depend upon the mineral composition, alter the solubility and vulnerability of the dust particle to wet scavenging. We defer representation of this dependence to a future study . . . .”

We have also added this discussion to the companion article. In the conclusions (p. 26, last paragraph), we briefly note our future plan to incorporate these processes.

P 18, 20-25: It would be useful to discuss what physical processes could affect this ration. E.g., it can not change within one size bin, I believe. **(Page 3595, line 20-25)**

We add a brief discussion to the second paragraph of Sect. 5.3 (p.21, line 4). For minerals other than pure crystalline iron oxides, the ratio with respect to quartz is relatively constant along a trajectory, as noted by the reviewer.

> “Like mineral fractions, mineral ratios will evolve downwind of the source region . . . .”

P 21, 13-20: What does control the emission of small particles? Is it availability of clay fraction in the soil layer or it is hydrodynamic entrainment that is less effective for small particles? Please explain. **(Page 3598, lines 14-22)**

Aerodynamic entrainment is inefficient for clay-sized particles because the cohesive force per unit area is large. These small particles mainly enter the atmosphere through bombardment by larger particles or else disintegration of larger particles. Kok (2011) gives a physical argument as to why the mass distribution of emitted particles is weighted toward larger sizes. The point that we wanted to reiterate in the conclusions is that the soil texture data are based on soils that are fully dispersed by wet sieving. This dispersion is much more destructive of soil aggregates than saltation and sandblasting which (according to measurements and brittle fragmentation theory) allows some of the smaller (silt-sized) aggregates to persist as aerosols. This is discussed in the opening paragraph of the conclusions (p. 23).

> “Minerals like phyllosilicates that are aggregates of smaller soil particles are almost exclusively observed at clay sizes after wet sieving, despite aerosol measurements showing greater phyllosilicate mass at silt diameters (eg. Kandler et al., 2009). This suggests that many of the aggregates that are destroyed during wet sieving would resist complete disintegration during wind erosion of the original, undispersed soil. “

There is also a fuller discussion in Sect. 2.1.2 of the companion article.

P 23, 13-17: Aging of dust is an important process especially for iron oxides. Do you account for it? **(Page 3600, lines 18-25)**

No; this is one of our next projects. We note our general neglect of particle transformations (but not for iron specifically) in Sect. 2.2 (p. 9, penultimate paragraph), the companion article, and briefly within the conclusions (p. 26, last paragraph).

Response to the Comments by Reviewer #2

This article provides an extensive evaluation of the model for size and mineralogy- resolved dust emission presented in part 1. The authors construct an impressive compilation of measurements, from about 60 studies, making for a detailed evaluation. I have only a few comments, and recommend that the article be published after the authors address them.
It would be helpful to include a comparison against the results of Scanza et al. (2015), who use some of the same measurements to evaluate their model for mineralogy-resolved dust emission. Can the authors discuss the effects of the purported improvements over this recent study? Do the additional processes they include actually im- prove the simulation?

We have done calculations to understand the difference between the two methods. However, we feel that this comparison is beyond the scope of the current article, so we are planning a future manuscript on this topic.

I found the discussion section quite tedious to read, in part due its length. I would suggest improving the writing in this section, for instance by adding more sub-headings.

We appreciate this suggestion. In response, we have separated the results presented in Section 5 into a number of subsections that are limited to the discussion of a single figure or topic. We hope this new organization makes it easier for the reader to recognize our main points.

Response to the Comments by Paola Formenti

Authors shoudl include the following paper for data comparison : Formenti, P., Caquineau, S., Desboeufs, K., Klaver, A., Chevaillier, S., Journet, E., and Rajot, J. L.: Mapping the physico-chemical properties of mineral dust in western Africa: mineralogical composition, Atmos. Chem. Phys., 14, 10663-10686, doi:10.5194/acp-14-10663-2014, 2014.'

Thanks for pointing us to this paper. We noticed that the surface concentration measurements at Banizoumbou, Niger, which are analyzed in that paper are the same data as in Formenti et al. (2008). Those measurements are included in our evaluation. We have cited the more recent study in the conclusions (p. 26, line 1):

> "These refinements can be complemented with studies that map the mineral composition of specific sources (Formenti et al., 2014b)."

References

Arnold, E., Merrill, J., Leinen, M., and King, J.: The effect of source area and atmospheric transport on mineral aerosol collected over the North Pacific Ocean, Global and Planetary Change, 18, 137–159, doi:10.1016/S0921-8181(98)00013-7, http://dx.doi.org/10.1016/S0921-8181(98)00013-7, 1998.

Claquin, T., Schulz, M., and Balkanski, Y. J.: Modeling the mineralogy of atmospheric dust sources, J. Geophys. Res., 104, 22,243–22,256, doi:10.1029/1999JD900416, http://dx.doi.org/10.1029/1999JD900416, 1999.

Engelbrecht, J. P., McDonald, E. V., Gillies, J. A., Jayanty, R. K. M., Casuccio, G., and Gertler, A. W.: Characterizing Mineral Dusts and Other Aerosols from the Middle East—Part 1: Ambient Sampling, Inhalation Toxicology, 21, 297–326, doi:10.1080/08958370802464273, http://dx.doi.org/10.1080/08958370802464273, 2009.

Formenti, P., Rajot, J. L., Desboeufs, K., Caquineau, S., Chevaillier, S., Nava, S., Gaudichet, A., Journet, E., Triquet, S., Alfaro, S., Chiari, M., Haywood, J., Coe, H., , and Highwood, E.: Regional variability of the composition of mineral dust from western Africa: Results from the AMMA SOP0/DABEX and DODO field campaigns, J. Geophys. Res., 113, D00C13, doi:10.1029/2008JD009903, http://dx.doi.org/10.1029/2008JD009903, 2008.

Jeong, G. Y., Kim, J. Y., Seo, J., Kim, G. M., Jin, H. C., and Chun, Y.: Long-range transport of giant particles in Asian dust identified by physical, mineralogical, and meteorological analysis, Atmos. Chem. Phys., 14, 505–521, doi:10.5194/acp-14-505-2014, http://dx.doi.org/10.5194/acp-14-505-2014, 2014.

Journet, E., Balkanski, Y., and Harrison, S. P.: A new data set of soil mineralogy for dust-cycle modeling, Atmos. Chem. Phys., 14, 3801–3816, doi:10.5194/acp-14-3801-2014, http://dx.doi.org/10.5194/acp-14-3801-2014, 2014.

Kandler, K., Benker, N., Bundke, U., Cuevas, E., Ebert, M., Knippertz, P., Rodríguez, S., Schütz, L., and Weinbruch, S.: Chemical composition and complex refractive index of Saharan Mineral Dust at Izanã, Tenerife (Spain) derived by electron microscopy, Atmospheric Environment, 41, 8058–8074, doi:10.1016/j.atmosenv.2007.06.047, http://dx.doi.org/10.1016/j.atmosenv.2007.06.047, 2007.

Kandler, K., Schütz, L., Deutscher, C., Ebert, M., Hofmann, H., Jäckel, S., Jaenicke, R., Knippertz, P., Lieke, K., Massling, A., Petzold, A., Schladitz, A., Weinzierl, B., Wiedensohler, A., Zorn, S., and Weinbruch, S.: Size distribution, mass concentration, chemical and mineralogical composition and derived optical parameters of the boundary layer aerosol at Tinfou, Morocco, during SAMUM 2006, Tellus B, 61, 32–50, doi:10.1111/j.1600-0889.2008.00385.x, http://dx.doi.org/10.1111/j.1600-0889.2008.00385.x, 2009.

Kok, J. F.: A scaling theory for the size distribution of emitted dust aerosols suggests climate models underestimate the size of the global dust cycle, PNAS, 108, 1016–1021, doi:10.1073/pnas.1014798108, http://www.pnas.org/content/108/3/1016, 2011.

Lafon, S., Sokolik, I. N., Rajot, J. L., Caquineau, S., and Gaudichet, A.: Characterization of iron oxides in mineral dust aerosols: Implications for light absorption, J. Geophys. Res., 111, D21207, doi:10.1029/2005JD007016, http://dx.doi.org/10.1029/2005JD007016, 2006.

Leinen, M., Prospero, J. M., Arnold, E., and Blank, M.: Mineralogy of aeolian dust reaching the North Pacific Ocean 1. Sampling and analysis, J. Geophys. Res., 99, 21,017–21,023, doi:10.1029/94JD01735, http://dx.doi.org/10.1029/94JD01735, 1994.

Nickovic, S., Vukovic, A., Vujadinovic, M., Djurdjevic, V., and Pejanovic, G.: Technical Note: High-resolution mineralogical database of dust-productive soils for atmospheric dust modeling, Atmos. Chem. Phys., 12, 845–855, doi:10.5194/acp-12-845-2012, http://dx.doi.org/10.5194/acp-12-845-2012, 2012.

Perlwitz, J. P., Pérez García-Pando, C., and Miller, R. L.: Predicting the mineral composition of dust aerosols. Part I: Representing key processes, Atmos. Chem. Phys. Discuss., 15, 3493–3575, doi:10.5194/acpd-15-3493-2015, http://www.atmos-chem-phys-discuss.net/15/3493/2015/acpd-15-3493-2015.html, 2015.

Manuscript prepared for Atmos. Chem. Phys. Discuss.
with version 2014/09/16 7.15 Copernicus papers of the LaTeX class copernicus.cls.
Date: 6 September 2015

Predicting the mineral composition of dust aerosols – Part 2: Model evaluation and identification of key processes with observations

J. P. Perlwitz[1,2], **C. Pérez García-Pando**[1,2], **and R. L. Miller**[2,1]

[1]Department of Applied Physics and Applied Mathematics, Columbia University in The City of New York, New York, USA
[2]NASA Goddard Institute for Space Studies, New York, New York, USA

Correspondence to: J. P. Perlwitz (jan.p.perlwitz@nasa.gov)

Abstract

A global compilation ~~from~~ of nearly sixty measurement studies is used to evaluate two methods of simulating the mineral composition of dust aerosols in an Earth system model. Both methods are based upon a Mean Mineralogical Table (MMT) that relates the soil mineral fractions to a global atlas of arid soil type. The Soil Mineral Fraction (SMF) method assumes that the aerosol mineral fractions match ~~those~~ the fractions of the soil. The MMT is based upon soil measurements after wet sieving, ~~where soil aggregates are broken into smaller particles~~ a process that destroys aggregates of soil particles that would have been emitted from the original, undisturbed soil. The second method approximately reconstructs the ~~aggregates and size distribution of the original soil that is subject to wind erosion~~emitted aggregates. This model is referred to as the Aerosol Mineral Fraction (AMF) method because the mineral fractions of the aerosols differ from those of the wet-sieved parent soil, partly due to reaggregation. The AMF method remedies some of the deficiencies of the SMF method in comparison to ~~observation~~observations. Only the AMF method ~~restores phyllosilicate mass to~~ exhibits phyllosilicate mass at silt sizes, where they are abundant according to observations. In addition, the AMF quartz fraction of silt particles is in ~~closer~~ better agreement with measured values, in contrast to the overestimated SMF fraction. Measurements at ~~separate~~ distinct clay and silt particle sizes are shown to be more useful for evaluation of the models, ~~compared~~ in contrast to the sum over all particles sizes that is susceptible to compensating errors~~in~~, as illustrated by the SMF experiment. Model errors suggest that ~~apportionment~~ allocation of the emitted silt fraction of each mineral into the corresponding transported size categories is an important remaining ~~uncertainty. Substantial uncertainty remains in evaluating~~ source of uncertainty. Evaluation of both models and the MMT ~~due to~~ is hindered by the limited number of size-resolved measurements of mineral content that sparsely sample aerosols from the major dust sources. The importance of climate processes dependent upon aerosol mineral composition shows the need for global and routine mineral measurements.

1 Introduction

The effect of soil dust aerosols upon climate is ~~strongly~~ dependent upon the particle mineral composition (see Perlwitz et al., 2015, and references therein). Despite ~~this~~regional variations in soil mineral content, the radiative and chemical properties of dust aerosols are nearly always assumed by Earth system models to be globally uniform~~and independent of their source region~~.

Claquin et al. (1999) provided the first global estimate of soil mineral content by relating it to soil type, whose regional distribution is given by the Digital Soil Map of the World (DSMW; FAO, 2007; FAO/IIASA/ISRIC/ISSCAS/JRC, 2012). Nickovic et al. (2012) and Journet et al. (2014) extended this approach by including additional ~~soil types, measurements~~ measurements, soil types and minerals. Deriving the mineral composition of emitted aerosols from the soil composition presents additional challenges. ~~Claquin et al. (1999) note that measurements of soil type~~ Soil measurements that are the basis of global datasets are based on ~~wet sedimentation (or "wet sieving ") techniques~~ fully dispersive techniques like wet sieving that disturb the soil samples, breaking the aggregates ~~that are~~ found in the original ~~, undispersed~~ soil that is subject to wind erosion (Claquin et al., 1999). Wet-sieving alters the soil size distribution, replacing aggregates with a collection of smaller ~~and relatively loose~~ particles (Shao, 2001; Choate et al., 2006; Laurent et al., 2008). In the absence of measurements of the undisturbed or minimally disturbed soil, studies have assumed that the size distribution of the emitted minerals ~~resemble those~~ resembles that of the wet-sieved parent soil (Hoose et al., 2008; Atkinson et al., 2013; Journet et al., 2014). ~~An additional~~ In fact, measurements show that emitted aerosols contain aggregates of soil particles, and that the emitted size distribution is shifted toward larger diameters compared to the wet-sieved soil (e.g. Kok, 2011). This contrast between the size distribution of the fully-dispersed soil and the emitted aerosol is important for the aerosol mineral content and lifetime.

A second challenge is how to treat particles that are combinations of different minerals. For example, iron oxides are often observed as small impurities attached to particles comprised ~~predominately~~ predominantly of other minerals (~~e.g.~~ Scheuvens and Kandler, 2014). These mixed particles have roughly half the density of pure iron oxides, and thus carry iron farther downwind of its source.

Finally, refinement of models is challenged by limited global measurements of size-resolved aerosol composition. Much of the available measurements are from field campaigns or ship cruises of limited duration, while changes in the sampling and analysis methods through time have ~~resulted in~~ contributed additional uncertainty.

We address the first two challenges in a companion paper (Perlwitz et al., 2015), where we describe a new approach to ~~estimate~~ estimating aerosol mineral content. ~~by extending the method that provides the composition of a wet-sieved soil (Claquin et al., 1999). We reconstruct the undispersed size distribution of the original soil that is subject to wind erosion, and apply an empirical constraint upon the relative emission of clay and silt that further differentiates the soil and aerosol mineral content.~~We use brittle fragmentation theory (Kok, 2011) and aerosol measurements (Kandler et al., 2009) to calculate the aerosol mineral composition and its size distribution in terms of the mineral fractions of the wet-sieved soil provided by Claquin et al. (1999).

We also propose a method for mixing minerals with small impurities of iron oxides~~. In the companion article, we compare regional variations of mineral emission and concentration calculated by our modeland a baseline model that assumes the aerosol mineral fractions are identical to those of the wet-sieved parent soil. We perform a limited comparison to size-resolved measurements from North Africa, showing that our extensions bring the model into better agreement~~, which we call "accretions". In our model, iron oxides can travel either in pure crystalline form or as accretions internally mixed with other minerals.The distribution of the two forms of iron oxide is based on the degree of weathering that creates iron oxides in the soil (McFadden and Hendricks, 1985; Shi et al., 2011).

In this article, we compare our ~~models'~~ calculation of aerosol mineral content to a new global compilation of observations from almost sixty citations. In Sect. 2, we summarize our new modeling approach and the simulations performed with the NASA Goddard Institute for Space Studies (GISS) Earth System ~~ModelE~~ModelE2, whose details can be found in the companion article (Perlwitz et al., 2015). Section 3 presents our global compilation of aerosol measurements for model evaluation (that is available in Table S1 of the Supplement), while Sect. 4 describes the evaluation approach. In Sect. 5, ~~we discuss the results of the evaluation in terms of mineral fractions, ratios and size distribution.~~ we show that agreement with the global compilation of aerosol measurements is improved by accounting for the modification of the mineral fractions of the parent soil during emission. Our conclusions ~~and recommendations~~ are presented in Sect. 6.

2 ~~Model simulations~~Description of model and experiments

Simulations are performed with the ~~NASA GISS ModelE using a resolution of 2° latitude by 2.5° longitude covering the years 2002 to 2010. This period was chosen to coincide with the detailed measurement record at Izaña that is analyzed separately (Pérez García-Pando et al., 2015), but overlaps with many of the measurements used for evaluation in the present study. The horizontal winds at each level of the model are nudged every six hours toward the NCEP reanalyzed values (Kalnay et al., 1996). This increases the resemblance of model transport to that observed so that the mineral fractions simulated at the observing sites are more strongly dependent upon our treatment of aerosol emissionand removal. Similarly, we prescribe atmospheric composition, sea surface temperature and sea ice based upon observed values (e.g. Rayner et al., 2003). Dust radiative forcing is calculated from a climatological background distribution whose particle optical properties are assumed to be regionally invariant. Calculation of radiative forcing by the individual minerals included in this study is deferred to a later time~~CMIP5 version of the NASA GISS Earth System ModelE2 (Schmidt et al., 2014), whose dust aerosol module is modified to incorporate individual minerals. In this section, we summarize the calculation of the size-resolved mineral fractions at emission. while describing the dust aerosol module and the configuration of the simulations. For a full description, the reader is referred to the companion paper (Perlwitz et al., 2015).

2.1 Emitted mineral fractions: baseline and new approaches

Two ~~experiments will be~~ simulations are compared to our compilation of observations. ~~These experiments are more fully described in Perlwitz et al. (2015), but their main features are given here. In the baseline or control experiment, the soil mineral fractions~~ The control or “baseline” simulation assumes that the emitted mineral fractions are identical to those of the wet-sieved parent soil~~are calculated using a global atlas~~; this calculation is referred to as the Soil Mineral Fraction (SMF) method. The soil (and thus the emitted) mineral fractions are calculated by combining the Mean Mineralogical Table (MMT; Claquin et al., 1999; Nickovic et al., 2012) with global atlases of arid soil type ~~and the Mean Mineralogical Table (MMT)constructed by Claquin et al. (1999). The~~ (Digital Soil Map of the World - DSMW; FAO, 1995, 2007) and soil texture (Hybrid STATSGO/FAO; FAO/IIASA/ISRIC/ISSCAS/JRC, 2012; NRCS Soil Survey Staff, 2012).

The MMT provides the fractional abundance for eight minerals within the clay and silt-size ranges of the soil as a function of arid soil type. For the clay-size range (whose diameters are less than 2 µm), the MMT gives the ~~soil fractions~~ fraction of phyllosilicates (illite, kaolinite, and smectite) along with quartz and calcite~~in the clay-size range (whose diameters are less than 2 µm)~~. Similarly, at silt sizes (with diameters between 2 and 50 µm), the MMT gives the ~~fractions~~ fraction of quartz and calcite along with feldspar, gypsum and hematite. According to the MMT, hematite is present in the soil only at silt sizes. Aerosol measurements show this mineral to be present at both clay and silt sizes (Lafon et al., 2006); Kandler et al., 2007; Engelbrecht et al., 2009; Jeong et al., 2014), so we extend the size range of emitted hematite to include clay sizes. Given the limited measurements of this mineral in soil samples, we follow Nickovic et al. (2012), and assume for simplicity that the hematite fraction at clay sizes in identical to the silt fraction provided by the MMT. In the remainder of this study, we refer to ~~the latter mineral~~ hematite more generally as “iron oxide”. This is because our treatment of hematite could apply to other iron minerals like goethite that are included in more recent and refined versions of the MMT (e.g. Journet et al., 2014). Similarly, we refer to calcite more generally as “carbonate”. ~~Following Nickovic et al. (2012),~~

~~we extend iron oxides into the clay-sized range by assuming that their fraction is identical to their MMT value at silt sizes.~~

The mineral fractions provided ~~for each size class~~ by the MMT for each size category are combined with the mass fraction of each size ~~class~~ category provided by the ~~FAO~~ soil texture atlas. This gives the size-resolved mineral fractions of the wet-sieved soil at each location. ~~For our baseline experiment, we assume that the aerosol mineral fractions are identical to the soil mineral fractions that vary with the local soil type and texture. We refer to this experiment as the Soil Mineral Fraction (SMF) version.~~

After emission, the minerals are transported within five size classes with diameters extending between 0.1 and 32 µm. Clay-sized particles are transported in a single bin by ModelE2. For silt particles, the MMT gives the emitted fraction of each mineral summed ~~over the entire size range (~~between 2 and 50 µm~~)~~. It remains to distribute this fraction over the four ~~silt-size~~ silt categories transported by the model. ~~In the absence of size-resolved measurements of emission for individual minerals, we use the size distribution of surface concentration measured for each mineral~~ For each mineral, we allocate the emitted silt fraction to the model size categories using a normalized distribution derived from measurements of dust concentration at Tinfou, Morocco ~~by Kandler et al. (2009). The size distribution of surface concentration is influenced by deposition, and~~ (Kandler et al., 2009). In the SMF method, this allocation uses a distribution that is identical for all minerals.

Dust at Tinfou is measured after transport from the source, when the largest particles are removed preferentially by gravitational ~~setting. Thus, our use of surface concentration to apportion emission within the silt size category may underestimate emission of the largest sized particles. In fact,~~ settling. Perlwitz et al. (2015) show that our model underestimates the aerosol fraction ~~of~~ within the largest silt-size category for all minerals at Tinfou ~~for the largest silt size category~~ (their Fig. ~~18~~17), suggesting that ~~our emission of~~ emission at this size is underestimated. Because the ~~size-resolved fractions derived from surface concentration are~~ relative size dependence of emission is normalized, underestimated emission of the largest silt particles ~~would correspond~~ corresponds to an overestimate of the emitted fraction of the ~~smallest~~ smaller silt particles. We will return to ~~the effect of~~ this potential bias when we evaluate the model with observations.

~~Our second experiment is movitated~~ The allocation of silt-sized emission within the individual size categories transported by ModelE2 is empirical and based upon measurements at only a single location. It is difficult to test the validity of this allocation at other locations, given the paucity of size-resolved measurements of mineral fractions. At diameters above roughly 20 µm (below which brittle fragmentation theory provides a good fit to available measurements), the emitted size distribution is a complicated function of wind speed and soil characteristics (Alfaro and Gomes, 2001; Grini et al., 2002). However, the increase of emitted mass with increasing particle size that is exhibited at Tinfou (cf. Fig. 3 of the companion article, second panel from left) is probably a robust result of the decreasing wind speed threshold for emission as a function of diameter within this size range (Iversen and White, 1982).

Our second simulation is motivated by measurements showing significant differences between the size-resolved mineral fractions of ~~the~~ wet-sieved ~~soil and the resulting~~ soils and aerosol concentration. ~~We extend the baseline method by first reconstructing the original size distribution of the soil prior to wet sieving. We reconstruct silt-sized aggregates in proportion to the clay-sized minerals present in the wet-sieved soil, using an empirical coefficient of proportionality γ that controls the amount of reaggregation. The reconstructed silt fraction is thus a combination of silt-sized particles~~ This simulation is referred to as the Aerosol Mineral Fraction (AMF) method to emphasize the difference between the aerosol and soil mineral fractions (in contrast to the SMF where these fractions are assumed to be identical). This difference results because wet sieving is more destructive of aggregates of soil particles than mobilization of the original, undispersed soil, where many of the aerosols are comprised of aggregates that resist complete disintegration during emission. Brittle fragmentation theory provides a physically based method for reconstructing the emitted size distribution from the distribution measured after wet sieving (Kok, 2011). The emitted silt fraction consists not only of silt particles present in the wet-sieved soil ~~along with~~, but also aggregates that were ~~converted~~ broken during wet sieving into clay-sized ~~particles~~

~~during sieving. As a consequence, phyllosilicate~~ fragments. In the AMF simulation, we reaggregate these fragments heuristically. For each mineral, the emitted silt fraction is comprised of silt particles in the wet-sieved soil augmented in proportion to the mineral's wet-sieved clay fraction. The degree of augmentation is prescribed through a proportionality constant γ. We set $\gamma = 2$ for our reference AMF simulation, although we have not made much effort to find an optimal value of this parameter. Results with $\gamma = 0$ are also shown to illustrate the physical origin of the size and regional distributions of minerals within the AMF experiment, and their contrast with respect to those of the SMF method. The only mineral that is not reaggregated in the AMF simulation is quartz, whose physical integrity is assumed to be large enough to prevent disintegration during wet sieving. One effect of reaggregation is to introduce clay minerals (illite, kaolinite and smectite) ~~that are nominally "clay" minerals are more prevalent~~ as aerosols at silt sizes~~, consistent with aerosol measurements (Kandler et al., 2009), even though they are absent in a soil whose aggregates are dispersed by wet sieving~~. This introduction is consistent with observations (e.g. Kandler et al., 2009), and in contrast to the SMF simulation, where aerosols comprised of clay minerals are absent at silt sizes, as prescribed by the MMT (Claquin et al., 1999).

~~In addition, we account for the transformation of the mineral fractions during the emission process. We constrain the emitted clay and silt-sized fractions with measured size distributions of aerosol emission that have been shown to be relatively invariant up to 20 µm for a variety of soils and wind conditions (e.g. Gillette et al., 1974; Sow et al., 2009; Kok, 2011). The measured fraction of emission at clay sizes is also used to extend the size range of emitted~~ Conversely, the MMT provides the fraction of feldspar and gypsum ~~into clay-sized diameters. (These~~ only at silt sizes, even though aerosol measurements show that these minerals are present ~~only at silt sizes in the MMT and the SMF model.) Our extensions of the SMF method result in aerosol mineral fractions that are different from fractions of the wet-sieved parent soil. As such, we refer to our new method as the Aerosol Mineral Fraction (AMF) experiment. Apportionment of emitted silt into the corresponding four size categoriestransported by the model is prescribed using the fractional size-distribution of~~

~~surface concentration measured at Tinfou, as in the SMF method~~at both clay and silt sizes (Leinen et al., 1994; Arnold et al., 1998; Kandler et al., 2007, 2009). We combine the silt fraction of feldspar and gypsum provided by the MMT along with the emitted ratio of clay and silt-sized particles provided by brittle fragmentation theory and the normalized volume distribution derived from Kandler et al. (2009) to extend the emission of these minerals to clay sizes. Details are provided in the companion article (Perlwitz et al., 2015).

To apportion the emitted silt fraction of the AMF simulation into the ModelE2 transport categories, we combine the size distribution derived from brittle fragmentation theory (that is valid for diameters below roughly 20 µm) with the empirical volume fraction derived for each mineral. We calculate this fraction for each mineral separately (cf. Fig. 4 of the companion article), in contrast to the SMF simulation, where we use a single distribution averaged over all minerals. One consequence is that quartz emission in the AMF simulation is shifted toward larger diameters, compared to the SMF simulation. This has the effect of reducing the quartz fraction in the AMF experiment, due to the higher gravitational settling speed of larger particles.

Finally, for the AMF experiment, we ~~form internal mixtures of minerals with small impurities of iron oxides . These host minerals~~ allow iron oxides to be emitted not only in their pure, crystalline form, but additionally as impurities mixed with other minerals. These mixtures are important for transporting iron far from its source, because pure iron oxides are more dense and vulnerable to gravitational removal than most ~~minerals comprising dust aerosols~~other minerals that contain small inclusions or accretions of iron oxides. We assume that the ~~mixture~~ partitioning of iron oxides ~~within other minerals is smaller where the soil is enriched in total iron oxide, a heuristic attempt to identify regions of enhanced~~ into mixtures and pure crystalline forms depends upon the soil fraction of iron oxides compared to the other minerals (as given by the MMT, including our extension to clay sizes). Soils enriched in iron oxides are assumed to be highly weathered, with a greater abundance of the pure, crystalline form (McFadden and Hendricks, 1985; Shi et al., 2011). As noted in the companion article, this is a heuristic representation of the effects of soil weathering that

~~creates pure crystalline iron oxides.~~ is more speculative than the remainder of the AMF method, and subject to future revision.

~~Our AMF model includes an empirical constant γ that controls the amount of aggregation of clay-sized particles in the wet-sieved soil into silt-sized emitted aerosols. We set $\gamma = 2$ for our reference AMF simulation, although we have not made much effort to find an optimal value of this parameter. Results with $\gamma = 0$ are also shown to illustrate the physical origin of the size and regional distributions of minerals within the AMF experiment, and their contrast with respect to the SMF method.~~

~~The global emitted mass of particles with diameters less than 32 µm for all experiments is scaled to be identical at 2224 Tg per year. However, in this article, we evaluate the relative proportions of the simulated minerals that are independent of the emission magnitude.~~

2.2 The dust aerosol module with mineral tracers

The dust aerosol module described by Miller et al. (2006) is modified here to represent each mineral (and its combination with iron oxides) as a separate prognostic variable within each of five size bins whose diameters range from 0.1 and 32 µm. The emitted mass of each mineral is the product of its emitted fraction, whose calculation is described above, and the total emission.

Dust sources are prescribed within topographic depressions (Ginoux et al., 2001), where vegetation is sparse and the soil particles that accumulate from erosion of the surrounding highlands are exposed to the force of the wind. (Vegetation is prescribed using surface roughness; Prigent et al., 2005.) Emission occurs when the surface wind speed exceeds a threshold that increases with soil moisture, following Shao et al. (1996). The surface wind includes contributions from wind gusts that are parameterized as described in Cakmur et al. (2004). In this article, we evaluate only the relative proportions of the simulated minerals; these are independent of the global magnitude of emission.

Dust removal results from wet and dry deposition. The latter includes gravitational settling and turbulent deposition in the surface layer (Wesely and Hicks, 1977; Koch et al., 1999) , with settling speeds that are proportional to mineral density (Tegen and Fung, 1994). All minerals have similar densities, except for iron oxides whose density is nearly twice the value of the other minerals (Table 8; Perlwitz et al., 2015).

Wet deposition has been updated since its description in Miller et al. (2006), and is now calculated consistently with other aerosol species (Bauer and Koch, 2005; Schmidt et al., 2006). Aerosol scavenging is proportional to dust solubility and now occurs both within and below clouds where there is precipitating condensate. Scavenging is offset by re-evaporation of cloud droplets and precipitation.

Measurements show that physical and chemical properties of aerosols evolve along their trajectory (cf. Baker et al., 2014). For example, phyllosilicates adsorb water (Navea et al., 2010), while heterogeneous uptake of precursor gases leads to sulfate and nitrate coatings on the particle surface. These modifications, which depend upon the mineral composition, alter the solubility and vulnerability of the dust particle to wet scavenging. We defer representation of this dependence to a future study and assume the solubility of each dust particle to be constant (50%) and identical for each mineral (Koch et al., 1999).

We also defer calculation of radiative forcing as a function of the aerosol mineral composition. As a result, radiative feedbacks between the mineral fractions and climate are disabled.

2.3 Simulations

Both the SMF and AMF simulations are performed with ModelE2 at resolution of 2° latitude by 2.5° longitude and 40 vertical levels. The period of 2002 through 2010 is simulated to coincide with detailed measurements at Izaña that are analyzed separately (Pérez García-Pando et al., 2015), but overlap with many of the measurements used for evaluation in the present study. The horizontal winds at each level of the model are relaxed every six hours toward the NCEP reanalyzed values (Kalnay et al., 1996). Relaxation occurs at all model levels (up to 10 hPa) with the globally uniform time scale of 100 s. Relaxation increases the resemblance of model transport to that observed so that the mineral fractions simulated at the observing sites are more strongly dependent upon our treatment of aerosol emission and removal than the calculated transport. Similarly, we prescribe sea surface temperature and sea ice based upon observed values (e.g. Rayner et al., 2003).

3 ~~Observational data~~Observations for model evaluation

We compiled measurements of mineral fractions of dust aerosols from almost sixty studies published between the 1960s and the present day that are described in Table 1 and available in Table S1 of the Supplement. Roughly one-third of the studies are in common with a recent compilation focusing on North African sources by Scheuvens et al. (2013). Our compilation includes measurements of ~~mineral fractions of~~ dust concentration and deposition, both from land stations and ship cruises. A few studies provide measurements of dust deposited in permanent snow fields (Windom, 1969; Gaudichet et al., 1992; Zdanowicz et al., 2006). Measurements are not equally distributed over all dust source regions, and mostly sample dust transported from North Africa, the Middle East and Asia (Fig. 1). Only two studies provide measurements downwind of southern African sources (Aston et al., 1973; Chester et al., 1971). No studies were found for dust from North America, while only one site is affected by the Australian dust plume (Windom, 1969). Generally, most of the measurements for aerosol mineral composition are in the Northern Hemisphere and there is underrepresentation of the Southern Hemisphere. Also, many of the measurements in earlier decades were confined to the relative proportions of phyllosilicates.

Methods to determine the mineral composition of dust aerosols have varied over time, and the measurements in our compilation that are based on various instruments and analytical methods contain different biases and uncertainties. Systematic studies of the mineral composition of atmospheric soil dust started in the 1960s, beginning with Delany et al. (1967), who intended to investigate cosmic dust. The mineral composition of airborne dust was usually determined from samples collected on suspended nylon mesh over land or ships (e.g., Prospero and Bonatti, 1969; Goldberg and Griffin, 1970; Parkin et al., 1970; Chester and Johnson, 1971b; Tomadin et al., 1984). Typically, the collection efficiency of the mesh ~~is~~ was assumed to be 50 % (Prospero and Bonatti, 1969), but the true value depends upon particle size and wind velocity (Chester and Johnson, 1971a). Parkin et al. (1970) determined a collection efficiency of 100 % for spherical particles with densities of 3 g cm^{-3} and particle diameters greater than 7 µm, with the efficiency decreasing to 50 % for diameters of 2 µm and null collection of particles with diameters below 0.5 µm. Thus, mesh collection introduces a bias towards larger dust particles, and potentially overestimates the fraction of minerals such as quartz, whose abundance peaks at large particle sizes. Other studies analyzed dust ~~fallen~~ deposited on ship decks (e.g., Game, 1964; Johnson, 1976) or ~~deposited~~ over land (e.g., Goldberg and Griffin, 1970; Tomadin et al., 1984; Khalaf et al., 1985; Adedokum et al., 1989; Skonieczny et al., 2011).

Since the 1990s, airborne dust has been more commonly sampled with other instruments, like high-volume air samplers (e.g., Zhou and Tazaki, 1996; Alastuey et al., 2005; Shi et al., 2005; Jeong, 2008; Shen et al., 2009) or low-volume air samplers (e.g., Gao and Anderson, 2001; Engelbrecht et al., 2009). These samples ~~extracted~~ extract dust from the air with polycarbonate or quartz microfibre filters (Shi et al., 2005), cellulose filters (Jeong, 2008), or other filters (Engelbrecht et al., 2009). The finest aerosol ~~particle~~ particles can get trapped in the quartz fibre filters before the sample is treated for the mineral analysis, a source of collection inefficiency and uncertainty (Alastuey et al., 2005).

The relative mass fractions of the collected minerals are often derived from X-ray diffraction (XRD) spectra (e.g., Prospero and Bonatti, 1969; Alastuey et al., 2005; Shi et al., 2005; Skonieczny et al., 2011). The wavelength of spectral peaks give information about elemental and mineral composition, while the mass fraction relative to other minerals is determined by area under the peak. Characterization of the area ~~of the peak~~ (rather than ~~its maximum) accounts for~~ the peak) increases the sensitivity to particle diameters less than 10 µm that cause peak broadening (Glaccum and Prospero, 1980).

XRD analysis is most effective for minerals with a regular crystal structure whose spectral peaks are well-defined. However, certain minerals like phyllosilicates consist of varying amounts of amorphous material whose ~~orientation can vary from particle to particle, complicating the interpretation of the sample diffraction~~ mass is difficult to quantify using

XRD (Formenti et al., 2008; Kandler et al., 2009). Among the various minerals considered in this study, the fraction of smectite is one of the most difficult to estimate. Its spectral peaks are small and can lie within the noise level of the XRD analysis (Glaccum and Prospero, 1980). This has been interpreted as the result of low concentration and poor crystallization (Leinen et al., 1994). ~~As a consequence, smectite is occasionally reported only in combination with illite (Shi et al., 2005; Shao et al., 2008).~~ This is additionally due to the frequent interleaving of smectite with illite and other minerals like chlorite, both in soils (Środoń, 1999) and aerosols (Shi et al., 2005; Lu et al., 2006), which can lead to misidentification of the individual phyllosilicates. As a consequence, smectite is occasionally reported only in combination with illite (Shi et al., 2005; Shao et al., 2008).

The composition of airborne particles is increasingly studied by scanning electron microscope (SEM) images of individual particles along with statistical cluster analysis of elemental composition (e.g., Gao and Anderson, 2001; Lu et al., 2006; Kandler et al., 2009; Engelbrecht et al., 2009). Both XRD and SEM measurements are disproportionately sensitive to composition on the particle surface, which may include coatings resulting from chemical reactions with other species, compared to the particle interior.

All the ~~observation data~~ observations used for our evaluation are based on measurements of the mineral fractions of dust aerosols at the surface. A few studies also provide aircraft measurements (Formenti et al., 2008; Klaver et al., 2011; Formenti et al., 2014b). Those data are not taken into consideration but will be included in future evaluation of simulated vertical profiles.

Because of the difficulty of comparing the uncertainty of different measurement methods, we weight all observations equally. As prognostic models of mineral composition become more common, we hope that mineral ~~attribution of~~ identification within aerosol samples becomes more uniform and routine.

4 Method of evaluation

A ~~major~~ challenge for model evaluation is the difference in record length between climate model output and the mineral observations. Deposition is measured over periods as short as a week. Measurements of surface concentration are based mostly on daily sampling, with reported values ~~from relatively~~ derived from few days. In contrast, the output from our model simulations consists of a continuous stream of data, from which monthly averages are calculated. Note that even though the model output could be archived at higher frequencies, e.g., every model day, a large discrepancy between the small sample sizes of many of the measurements and large samples from the model simulations would persist. The mineral fractions that we use for evaluation reflect the composition of the soil at the source region. These fractions are probably more consistent than the absolute concentration of the separate minerals used to form this ratio, at least in those remote regions where ~~one~~ a single source dominates the supply. Thus, measurements of mineral fractions from ~~only~~ a few days may be representative of the entire month. Closer to a source, the mineral fractions may be more variable, with episodic increases of quartz and other minerals that are abundant at large diameters during dust storms (cf. Fig. 10 from Kandler et al., 2009). An evaluation of the uncertainty created by the limited measurement duration ~~using daily model output~~ is planned for the future using daily model output.

For each reference providing measurements, we calculate a time average that can be compared to the model output. In some cases, we estimate a monthly average using daily measurements that are available for only a subset of the month. Our simulations cover only the nine years between 2002 and 2010, but some of the measurements date back to the 1960s. Our evaluation assumes that multi-decadal variability in the mineral fractions of dust aerosols at individual locations is small compared to the fractions themselves. A more thorough discussion of the sampling uncertainty in our comparison between the measurements and model is provided in the Appendix.

We simulate only eight minerals in our model. However, measurements may include additional minerals that are not simulated. Other measurements ~~do~~ may not include all of the simulated minerals. (For example, Kandler et al. (2009) does not distinguish smectite from the other phyllosilicates.) To make the measured and simulated mineral fractions comparable, we recalculate the fractions at each individual data point using only minerals present in both the measurements and the model. We caution that this renormalization can be misleading if some minerals that contribute to the total dust mass were simply not reported. (The mineral fraction measurements compiled in Table S1 of the Supplement include all reported minerals, including both those simulated and those omitted from the ~~ModelE~~ModelE2.)

To account for different size ranges of the model and measurements, we ~~interpolated~~ interpolate the mass fractions from the model size bins to the size range of the measurements. For measurements of total suspended particles (TSP), we compare to the sum over the entire model size range. Since this range extends only to 32 µm, this can lead to a positive bias in the observations for minerals like quartz that are more abundant at larger particle sizes, particularly at measurement locations near dust sources.

We ~~compared~~ compare the measured and simulated mineral fractions and ratios using scatter plots. We calculate the normalized bias (nBias) and normalized root mean squared error (nRMSE). Normalization was done by dividing the statistic by the average of the observed values used in each scatter plot. The number of paired data points (N) from the measurements and the simulations is also provided with each scatter plot. These summary statistics are computed without weighting: for example, with respect to the number of measurements used to compute the average value of each study. Such precision seems illusory given the incommensurate analytical uncertainty of different measurement types discussed in Sect. 3. Our goal is not to provide a detailed statistical analysis using these metrics but to help identify robust improvement or deterioration of the AMF results compared to the SMF method.

Our evaluation compares measurements from a specific location to the value at the corresponding grid box. In the case of ship cruises, we use the average along the cruise trajectory within each ocean, forming a model average with the corresponding sequence of grid boxes. Our comparison assumes that the grid size of the model is sufficient to resolve spatial variations of the measurements. This is not always the case, particularly near dust sources that are often geographically isolated resulting in strong spatial contrasts of concentration (e.g. Prospero et al., 2002). For example, we discuss below measurements by Engelbrecht et al. (2009) and Al-Dousari and Al-Awadhi (2012), who find large variations in mineral ratios with respect to quartz at nearby locations in the Middle East. Some of these measurements are within a single grid box and thus impossible to resolve with the model.

5 Evaluation of the predicted mineral fractions

In a companion paper (Perlwitz et al., 2015), it is shown that the AMF method brings the model into better agreement with ~~size-resolved measurements of surface concentration~~ size-dependent surface concentration derived from measurements at Tinfou, ~~Morroco~~Morocco (Kandler et al., 2009). ~~In contrast to the SMF experiment, the~~ The AMF method reproduces the observed large mass fraction of phyllosilicates at silt sizes and reduces the quartz fraction, ~~bringing the latter into agreement with measurements~~in contrast to the SMF experiment (~~Fig. 18~~Fig. 17 in Perlwitz et al., 2015). The AMF method also introduces feldspar and gypsum at clay sizes, despite their exclusion from the MMT and SMF experiment. Both experiments underestimate all mineral fractions at the largest model size category, possibly because the emitted silt is distributed among the corresponding four model size categories using size-resolved measurements ~~of surface concentration~~ following transport from the source and after removal of the largest particles by gravitational settling, as described in Sect. 2.1.

Below, we extend the evaluation of ~~the size-resolved mineral fractions by~~ both methods to the global scale. We calculate mineral fractions that are the ratio of the mass of each mineral to the sum over all minerals. Alternatively, we consider the ratio of specific mineral pairs. The mineral mass is derived from surface concentration or deposition, depending upon the measured quantity.

5.1 Seasonal cycle of mineral fractions

Only a few locations have measurements at multiple times throughout the year, ~~although~~ and these are generally insufficient to resolve the seasonal cycle. We use these measurements for comparison to the model that at some locations exhibits a seasonal shift in the predominant mineral.

Figure 2 compares the simulated seasonal cycle of the phyllosilicate fraction to measurements at Barbados (Delany et al., 1967) and the Pacific (Leinen et al., 1994; Arnold et al., 1998). The fraction is defined relative to the sum of minerals that are present in both the model and measurements within the same size class. At Barbados, the illite-smectite and kaolinite fractions calculated by the models show contrasting seasonal cycles, driven by the seasonal shift of the Intertropical Convergence Zone (ITCZ) and the Trade Winds over the North Atlantic (Moulin et al., 1997). During summer, dust is preferentially transported from northern African sources enriched in illite and smectite, in contrast to winter, when dust is emitted from sources farther south containing higher amounts of kaolinite (Caquineau et al., 1998). Both experiments calculate mineral fractions that are consistent with the measurements, although the uncertainty due to the small sample size hampers a robust evaluation.

Over the Pacific, both the SMF and the AMF experiments show similar illite-smectite and kaolinite fractions at clay sizes that are consistent with the observations. The slightly smaller AMF fraction of phyllosilicates results from the addition of feldspar and gypsum at clay sizes that comes at the expense of the phyllosilicate fraction. (This difference between the AMF and SMF treatments of phyllosilicates is obscured in the Barbados measurements ~~,~~ because feldspar and gypsum are not measured and are thus excluded from our reconstruction of the total dust mass at clay sizes.) At silt sizes, the simulated AMF fraction of phyllosilicates that is observed at the Pacific locations is entirely absent in the SMF experiment, highlighting the importance of reconstructing the ~~phyllosilicate mass disaggregated~~ emitted phyllosilicate mass comprised of soil aggregates that are almost totally disintegrated during wet sieving of the soil samples. There is the suggestion that the kaolinite fraction is overestimated by the model at both clay and silt sizes, a discrepancy that is found at other locations, as will be discussed below.

Figure 3 compares the simulated seasonal cycle of feldspar and quartz in the Pacific to ship measurements. Both the AMF and SMF methods predict similar quartz fractions in the clay size range that are close to the observed values. However, the AMF method is in much better agreement with the measurements at silt diameters, whereas the SMF experiment overestimates the quartz fraction by nearly fourfold. Figures 2 and 3 show that the SMF overestimation of the quartz fraction at silt sizes at the expense of phyllosilicates is not limited to Tinfou and more generally, to the vicinity of source regions. The improved agreement of the AMF method results from the reintroduction of phyllosilicate mass into silt sizes through reaggregation, which has the effect of reducing the quartz fraction.

For feldspar, the AMF method reproduces the clay-size fraction of most measurements, in contrast to the SMF experiment which omits feldspar at this size. At silt diameters, both experiments are consistent with the measurements, owing in part to their large uncertainty.

5.2 Global evaluation of mineral fractions

We summarize the model performance by comparison to a global distribution of measurements at silt and clay diameters, respectively (Figs. 4 and 5~~, respectively~~) as well as ~~its~~ their sum over the entire model size range (the “bulk” composition: Fig. 6).

5.2.1 Mineral fractions in the silt size range

Figure 4 compares the measured and modeled fractions of phyllosilicate and quartz at silt sizes. The measurements cover various regions of the Northern Hemisphere, such as the northern and eastern Pacific (Leinen et al., 1994; Arnold et al., 1998), East Asia (Jeong et al., 2014), the Middle East (Ganor et al., 2000), the eastern Atlantic (Kandler et al., 2007), West Africa (Enete et al., 2012), and northwestern Africa (Kandler et al., 2009). Although there are ~~few~~ fewer measurements restricted to the silt size range~~(~~, compared to particle mass (PM) measurements that sum all diameters up to a prescribed limit~~)~~, measurements of these particular minerals are relatively abundant.

At silt diameters, the SMF method systematically overestimates the observed quartz fraction while entirely excluding the phyllosilicates (Fig. 4, top row). As shown previously, this feature is largely corrected by the AMF method (Fig. 4, middle row), as clay-sized soil particles are reaggregated ~~toward~~ for emission at silt sizes at the expense of the quartz fraction. The importance of reaggregation to the improved performance of the AMF method is shown by the experiment where the reaggregation parameter γ is set to zero (Fig. 4, bottom row). In the absence of reaggregation, quartz is overestimated and the phyllosilicates are underestimated, replicating the biases of the SMF experiment.

Even with reaggregation, the AMF method tends to underestimate illite at silt sizes, while overestimating kaolinite and smectite (the latter not shown). These errors could result from the mineral fractions prescribed by the MMT at silt sizes, but also from the MMT clay fractions due to reaggregation. Combinations of illite with the other phyllosilicates show better agreement. ~~This reveals compensating model biases, although the improved agreement of the combinations may also result from the observational challenge of distinguishing minerals like illite and smectite, and thus the more confident measurement of their combined mass fraction.~~

5.2.2 Mineral fractions in the clay size range

Figure 5 shows ~~similar~~ that the compensating model biases in the ~~clay-sized fractions~~ silt fraction of the individual ~~phyllosilicates~~phyllosilicate minerals are also present at clay sizes. The number of phyllosilicate measurements at clay diameters is relatively large, suggesting that these biases are robust. ~~All the~~ Both experiments have similar ~~biases at clay sizes, suggesting that the error is not the result of reaggregation or the prescribed size distribution of emission within the AMF method. The common biases of the individual phyllosilicates shown in Fig. 5~~ phyllosilicate biases, reflecting their common dependence upon the MMT clay fraction. Errors in the MMT could result from the challenge of distinguishing individual phyllosilicate minerals in the soil samples, as suggested by the improved agreement of the combined phyllosilicate fraction. Alternatively, this challenge could result from ~~the MMT that is used to prescribe the clay mineral fractions in all experiments, or the difficulty of distinguishing the individual phyllosilicates during measurement as mentioned above. However, other processes~~ errors and uncertainty in the aerosol measurements used to evaluate the model. Processes that are not represented in our model ~~could~~ will also contribute to the bias. For example, ~~we do not represent the preferential gravitational settling and wet removal of smectite during transportthat results from its~~ the solubility of dust particles and their vulnerability to wet removal is assumed constant during transport, even though minerals like smectite (that are overestimated compared to illite) have a large hygroscopic capacity ~~(Singer et al., 2004), an omission that would contribute to overestimation~~ and take up water preferentially (Frinak et al., 2005).

All three experiments show good agreement of the quartz fraction at clay sizes (Fig. 5). Measurements also show that feldspar is present at this size despite its omission by the SMF method. The clay-sized feldspar in the AMF and AMF ($\gamma = 0$) experiments is calculated using the MMT silt fraction of this mineral ~~.~~ along with the observed ratio of emitted clay to silt (Perlwitz et al., 2015, Eq. 14). The lower clay-sized fraction obtained with the AMF method, which is in better agreement with the few observations available, is explained by the reduced fraction of silt-sized feldspar in this experiment due to the reaggregation of phyllosilicate mass into the silt-size range.

5.2.3 Mineral fractions in bulk dust

Bulk measurements of mineral composition ~~that~~ represent sums over all particle sizes, and are plentiful compared to measurements within individual size categories. Both the SMF and AMF methods produce similar bulk fractions of phyllosilicates (Fig. 6), with a small negative bias for illite and a positive bias for kaolinite and smectite as previously noted for the individual clay and silt sizes. These biases compensate when the phyllosilicates are considered together (Fig. 6, rightmost column), but the simulated range of fractions remains underestimated by the AMF method.

~~The nearly uniform simulated fraction of the combined phyllosilicates in the AMF experiment illustrates several potential sources of model error. The error is especially apparent at various locations within the Arabian Peninsula (rightmost column, green points) that are located near dust sources (Al-Dousari and Al-Awadhi, 2012). Many of these measurements are proximal and the large spatial contrasts are difficult to resolve with the model. Moreover, the measured deposition is predominately quartz and carbonate with roughly one-third of the total mass with diameters above 63 µm. Overestimate of the phyllosilicate fraction at these locations could be caused by the model's exclusion of particle diameters above 32 µm that causes the total model dust mass to be underestimated.~~

~~Both the SMF and AMF experiments are susceptible to these sources of error, but the latter shows the largest error. The AMF experiment is distinguished by reaggregration, making it especially sensitive to errors in the MMT mineral fractions or the clay-sized fraction of the soil. A more subtle error potentially comes from the apportionment of the emitted silt into the model size bins using observations of surface concentration. We have noted how both experiments underestimate the fraction of every mineral at the largest model silt diameter according to measurements at Tinfou. Correction of this error would reduce the emission of the smaller silt categories (because the apportionment does not change the total silt emission). For the AMF experiment, reduced phyllosilicate emission at the smaller silt sizes would justify increasing our empirical reaggregation parameter to return the model to good agreement with the observations in Fig. 4. That is, the phyllosilicate mass would remain largely unchanged at small silt sizes compared to the present AMF experiment, but emission of all minerals at larger sizes would increase, reducing the fraction of phyllosilicates compared to the total dust mass and bringing it closer to the measured value. A similar redistribution is suggested by measurements of elemental ratios at Tinfou, where potassium increases relative to silicon (Kandler et al., 2009). One interpretation is that feldspar is becoming more important compared to phyllosilicates as their diameters increase. This would result in a distribution of feldspar weighted toward larger silt sizes, in contrast to our current assumption that they share an identical distribution with phyllosilicates. These corrections would have the greatest effect near source regions~~

~~like the Arabian Peninsula (where the largest particles have not yet been depleted by gravitational settling) and for the AMF experiment, whose fractional emission of total dust at silt sizes is larger than the SMF fraction. The larger point is that near source regions, errors in our apportionment of silt emission have the largest effect, showing the value of size-resolved measurements of emission that distinguish between minerals.~~

With the exception of source regions and their vicinity, the AMF and SMF methods produce bulk fractions of both total phyllosilicates and quartz that are in good agreement with the measured values (Figs. 6 and 7). This agreement is in spite of clear biases in the SMF experiment ~~of both mineral fractions~~ at silt sizes (Fig. 4). ~~The~~ In the companion article, it is shown that the SMF simulation emits less total dust (ie. summed over all minerals) at silt diameters compared to the AMF method, while emitting more at clay sizes. Thus, the SMF method compensates ~~an excessive silt~~ for an excessive fraction of quartz at silt diameters with smaller silt emission~~compared to the AMF method~~. Similarly, the unrealistic restriction of phyllosilicates to clay sizes in the SMF experiments is offset by greater emission at these sizes. ~~Thus, SMF~~ SMF fractional biases within individual size categories (Figs. 4 and 5) are hidden by bulk measurements due to the compensation of these errors.

This compensation is disabled in the AMF experiment with $\gamma = 0$, showing the ~~spurious~~ origin of the spurious agreement of the SMF method with the bulk measurements. For $\gamma = 0$, reaggregation of phyllosilicate mass into the silt category is eliminated, resulting in ~~a quartz fraction~~ an overestimated quartz fraction that nearly identical to the SMF value ~~. However,~~ at this size (Fig. 4). Consequently, the bulk measured value of the quartz fraction is overestimated (Fig. 6, bottom row), because the emitted silt fraction is large compared to the SMF method (albeit consistent with the ~~default AMF experiment~~AMF simulation and measurements).

Conversely, fractional emission ~~of clay sizes remains~~ at clay sizes for $\gamma = 0$ is small compared to the SMF experiment~~in agreement with empirical measurements~~, consistent with the default AMF experiment. As a result, the bulk fraction of phyllosilicates is underestimated for $\gamma = 0$~~, while there is an overestimate of quartz (Figs. 6 and 7)~~. This shows the compensating effect of enhanced emission ~~of the clay fraction~~ at clay sizes in the SMF experiment that allows good agreement ~~of the total mass , despite biases~~ with the observed bulk mass of phyllosilicates, despite no emission at silt sizes.

All ~~three experiments show good agreement at the clay-size range for the quartz fraction (Fig. 5). Measurements also show that feldspar is present at this size despite its omission by the SMF method. The clay-sized feldspar in the AMF and AMF ($\gamma = 0$) experiments is constrained by the feldspar content in the silt size range and the observed ratio of emitted silt to clay (Perlwitz et al., 2015, Eq. 14). The lower clay-sized fraction obtained with the AMF method, which is closer to the small amount of observations available, is explained by the reduced mass of silt-sized feldspar in this experiment due to the reaggregation of phyllosilicate mass into the silt-size range.~~

~~All~~ the experiments exhibit negative biases for their fractions of carbonates, gypsum, and iron oxide (Fig. 7). These minerals are a relatively small fraction of the soil according to the MMT, and the common model bias suggests that the MMT values may be an underestimate (although the uncertainty of these fractions is large due to limited measurements). The underestimate of iron oxides may additionally result from the exclusion of goethite by the MMT, a mineral that contributes over half of the measured iron oxide at some locations (Shi et al., 2012; Formenti et al., 2014a; Journet et al., 2014). ~~The measurements~~

Measurements over the Arabian Peninsula (Al-Dousari and Al-Awadhi, 2012) indicate a negative bias of the carbonate fractions (Fig. 7, green dots), that may result from the model's truncated size range that is a poorer approximation near source regions, as ~~previously discussed~~discussed below.

~~The figures presented here are constructed from measurements that span either the entire aerosol size range or correspond to a single size category of the MMT. Figure 8 (along with Fig. S1 of the Supplement) compare the model mineral fractions to additional measurements that extend across both MMT size classes. These additional figures support the previous interpretations. However, Fig. 8 shows that all the models consistently overestimate the quartz fraction at~~ ~~PM_{10}~~ ~~(light blue dots). These measurements correspond to the Middle East near source regions (Engelbrecht et al., 2009), and provide additional evidence that the prescribed fractions of emission within the model silt categories are~~

~~underestimates at the largest sizes with corresponding overestimates at the smaller sizes. This overestimate is consistent with the PM_{10} errors that is largest for the AMF ($\gamma = 0$) experiment that combines the large quartz fraction of the SMF experiment (undiluted by phyllosilicate reaggregation) with the large fraction of emitted silt corresponding to the AMF experiment.~~

5.3 Ratios of mineral fractions

The mineral fractions with respect to total dust that are analyzed in the previous section ~~avoid the effect of~~ are unaffected by model errors in ~~total~~ global emission. For consistency, we ~~have~~ constructed the total dust mass using only minerals that are common to both the model and the specific measurement study. However, this construction introduces errors where measurements ~~include minerals (within total dust , for example)~~ of total dust include minerals that are not reported. By considering ratios of specifc pairs of minerals, we avoid this ambiguity, even though distinguishing individual minerals can be more uncertain than measuring the total dust mass.

~~The identification of quartz is relatively straightforward, and the mineral ratios with respect to quartz are shown in Fig. 9. The figure~~ Figure **8** shows mineral ratios with respect to quartz, whose abundance allows relatively certain identification and measurement. Like mineral fractions, mineral ratios will evolve downwind of the source region. Within a single size bin, minerals that are denser or more soluble than quartz will decrease their ratio due to their larger gravitational settling speed or wet scavenging efficiency. In our model, we include only the first effect, and only pure crystalline iron oxides have a density that is appreciably different from that of quartz. With the exception of iron oxides, mineral ratios with respect to quartz are fairly constant within each size category. This ratio changes only as the relative contribution of different size bins to the mineral mass within the measured size range evolves downstream.

Figure **8** reiterates model behavior that was illustrated by ~~previous figures of the mineral fraction~~ the mineral fractions with respect to the total ~~aerosol~~ dust mass. For example, in the SMF experiment, phyllosilicates are absent outside of the clay size range, in contradiction to measurements (leftmost column, orange dots). This error is largely fixed in the AMF experiment. ~~This improvement is the result~~ Again, this is a consequence of reaggregation, as shown by the AMF experiment with the reaggregation parameter γ set to zero (bottom row), where the model phyllosilicate fraction is zero at purely silt diameters (orange dots). At clay sizes (dark blue dots), both experiments give similar fractions, reflecting their common derivation from the MMT. Similarly, feldspar and gypsum in the SMF experiment are absent at clay sizes (dark blue dots) as a direct result of the MMT.

~~Figure 9 shows that all experiments consistently underestimate the range of observed mineral fractions.For every mineral, the largest observed value is greater than the model maximum. The extreme observed values typically correspond to PM$_{10}$ measurements (light blue dots), many derived from the Middle East (Engelbrecht et al., 2009). That the discrepencies are common to all experiments suggests that they do not originate from unique features of each experiment or their treatment of specific minerals other than quartz. The limited horizontal resolution of the model may be one source of error that prevents the reproduction of sharp gradients, especially close to source regions. Alternatively, the underestimated model range may result from the construction of the MMT that is designed to give *mean* mineral fractions that are approximately valid for all examples of a particular arid soil type instead of representing the variations among the examples. Alternatively, the model PM$_{10}$ fractions may be biased by excessive quartz below this diameter. We described above how this might be the result of misapportionment of the emitted silt fraction into the corresponding four size categories that are transported by the model.~~

Additional ratios with respect to minerals other than quartz are shown in Figs. S3 to S6 of the Supplement.

5.4 Sources of model error

The overestimated bulk fraction of combined phyllosilicates in the AMF experiment at various locations within the Arabian Peninsula (Fig. 6, middle row, right column, green points) illustrates potential sources of model error. The measurement sites are located near dust sources, where there are aerosols with large diameters outside the range transported by ModelE2. Al-Dousari and Al-Awadhi (2012) report that deposition at these sites is predominantly quartz and carbonate with roughly one-third of the total aerosol mass contributed by diameters above 63 µm. Overestimate of the phyllosilicate fraction at these locations could be caused by the model's exclusion of particle diameters above 32 µm that causes the total model dust mass to be underestimated.

Figure **9**, which compares mineral fractions within additional size ranges, illustrates other challenges of modeling mineral fractions near dust sources. All the simulations underestimate the quartz fraction of PM_{10} measured within the Middle East (left column, light blue dots) by Engelbrecht et al. (2009). This error is partly a consequence of apportioning emitted silt into the model size bins using measurements after transport. Preferential settling of the largest particles between the time of emission and measurement results in an underestimate of emission at this size. Correction of this error would reduce emission within the smaller silt categories that contribute to PM_{10}. This is because the apportionment does not change the total silt emission, so that an increase at the largest size must be balanced by a reduction elsewhere. Both the SMF and AMF experiments are susceptible to errors of silt apportionment, but the overestimate of the PM_{10} quartz fraction is largest for the AMF ($\gamma = 0$) experiment (Fig. **9**, bottom row). This experiment combines the large quartz fraction of the SMF method (undiminished by phyllosilicate reaggregation) with the large fractional emission of silt diameters corresponding to the AMF method.

All the experiments consistently underestimate the range of observed mineral ratios (Fig. **8**). This underestimate is partly a consequence of the MMT that is designed to give a *mean* mineral fraction that is approximately valid for all examples of a particular arid soil type instead of representing the actual variations within this soil type. The limited range may also result from the horizontal resolution of the model that prevents the reproduction of sharp gradients that are observed close to source regions, where the largest aerosols are removed rapidly by gravitational settling. The short lifetime of large particles results in measured spatial contrasts that are large and difficult to simulate, especially where the measurement sites are closely spaced, as in the study of Engelbrecht et al. (2009).

The single particle measurements of mineral fractions at Tinfou cannot distinguish the size distributions of the phyllosilicates and feldspars, which are thus assumed to be identical (Kandler et al., 2009). However, the increasing elemental ratio of potassium compared to silicon with increasing particle diameter suggests that feldspar is becoming more abundant compared to phyllosilicates within the model's largest transport bin. This suggests that the distribution of feldspar is in fact weighted toward larger silt sizes, in contrast to our current assumption that it shares an identical distribution with phyllosilicates. These corrections would have the greatest effect near source regions like the Arabian Peninsula (where the largest particles have not yet been depleted by gravitational settling) and for the AMF experiment, whose fractional emission of total dust at silt sizes is larger than the SMF fraction. The more general point is that near source regions, errors in our apportionment of silt emission have the largest effect.

6 Conclusions

In a companion article (Perlwitz et al., 2015), we define two methods of calculating aerosol mineral composition based upon the Mean Mineralogical Table (MMT) proposed by Claquin et al. (1999). The MMT ~~specifies~~ infers the mineral composition of both the clay and silt-sized fractions of the soil at each location using a global atlas of arid soil type. For the Soil Mineral Fraction (SMF) method, we assume that the emitted size distribution corresponds to the local soil texture, so that the emitted mineral fractions and their dependence upon size are identical to those of the parent soil. Both the MMT and soil texture are based upon measurements that follow wet~~-~~sieving of the soil sample, whereby soil aggregates are broken into smaller particles. ~~Because the emitted mineral fractions are sensitive to their size distribution within the soil, we define a second experiment called the Aerosol Mineral Fraction (AMF) method that attempts to compensate for this disaggregration by reconstructing the mineral fractions in the original, undisturbed soil that is subject to wind erosion.~~ Minerals like phyllosilicates that are aggregates of smaller soil particles are almost exclusively observed at clay sizes after wet sieving, despite aerosol measurements showing greater phyllosilicate mass at silt diameters (eg. Kandler et al., 2009). This suggests that many of the aggregates that are destroyed during wet sieving would resist complete disintegration during wind erosion of the original, undispersed soil. We define a second experiment based upon the Aerosol Mineral Fraction (AMF) method that allows contrasts between the size distributions of the wet-sieved soil and the emitted minerals. We propose a ~~simple and approximate reconstruction , where silt-sized~~ heuristic reconstruction of aggregates based upon brittle fragmentation theory, where aggregrates of phyllosilicates and other minerals are reintroduced at silt sizes in proportion to their abundance at clay sizes in the wet-sieved soil. ~~In addition, we use size-resolved measurements of emission to specify the ratio of emitted clay to silt-sized particles.~~ The emitted clay fraction is ~~observed to be~~ small, so that phyllosilicate aerosols in ~~AMF model originate largely~~ the AMF simulation are largely present at silt sizes as a result of reaggregation. ~~Because the fraction of emitted silt is fixed, the reintroduction of phyllosilicate aggregates at silt sizes reduces the emitted quartz fraction at this size.~~ The reintroduction of phyllosilicate aggregates at silt diameters reduces the emitted quartz fraction, because the fraction of emitted silt is fixed. Many of these aggregates are small enough to travel far from their source. However, the silt-sized mineral fractions of the wet-sieved soil include particles as large as 50 µm that remain suspended only within a short distance from the parent soil. We specify the emitted fraction of each mineral at these larger diameters by using an empirical size distribution derived from measurements of dust arriving at Tinfou, Morocco. By accounting for these larger diameters, our study extends the method of Scanza et al. (2015), who also use brittle fragmentation theory to calculate emission of the far-traveled particles.

To evaluate the two experiments, we compiled measurements from nearly sixty studies that are distributed both near and far downwind of major dust source regions. In spite of this extensive compilation, many key sources remain undersampled~~, and insufficient measurements are available~~. There are insufficient measurements to resolve the seasonal cycle of the mineral fractions and corroborate seasonal shifts of the dominant mineral calculated by the model that imply a change in ~~model~~ source region. For example, kaolinite that is abundant in the Sahel dominates model deposition at Barbados during Northern

Hemisphere winter, while an increase of emission in North Africa during the summer delivers more illite. In general, the uneven distribution of measurement sites and their limited duration ~~of operation~~ imposes a large uncertainty that allows us to robustly evaluate only the most general features of the experiments.

Nonetheless, we show that the AMF method addresses key deficiencies of the SMF experiment in comparison to measurements. In particular, AMF phyllosilicates (that are nominally “clay” minerals) are most abundant at silt sizes, while the silt fraction of quartz is reduced compared to the SMF value and ~~closer to~~ in better agreement with measurements. In spite of the ~~more realistic~~ unrealistic behavior of the ~~AMF~~ SMF method at silt sizes, both experiments show reasonable agreement with ~~the~~ measurements when the mineral fractions are summed over the entire size range~~is considered collectively~~. This is because the emitted clay fraction in the SMF experiment is ~~larger~~ large relative to the AMF experiment. This extra emission of clay-sized phyllosilicates in the SMF simulation compensates for the ~~SMF method’s absence of silt-sized phyllosilicates~~absence of these minerals at silt sizes. Similarly, the reduced fraction of emission at silt sizes in the SMF experiment compensates for its excessive quartz fraction. The fractional emission of clay and silt sizes in the SMF experiment is based upon the local soil texture ~~and~~ that is derived from measurements of the fully dispersed, wet-sieved soil. However, the large fraction of emitted clay-sized particles in the SMF method is inconsistent with ~~measurements showing~~ emission measurements that show a relatively small and regionally invariant ~~emission at clay sizes as assumed by the AMF~~emitted clay fraction (e.g. Kok, 2011). Thus, measurements of mineral fractions that ~~are sums~~ sum over all sizes do not distinguish between the AMF and SMF methods because of compensating errors in the latter that are more clearly distinguished by measurements limited to silt diameters. This is shown by a variation of the AMF experiment with reaggregation omitted ($\gamma = 0$)~~. Here,~~ , where silt-sized phyllosilicates are absent ~~and the quartz fraction is excessive, because the AMF emission at silt sizes is larger than the SMF value~~andthe mineral fractions compared poorly to bulk measurements.

The AMF method ~~similarly~~ extends feldspar into the clay size range, consistent with measurements. However, the bulk mineral fractions of carbonates, gypsum and iron oxides are underestimated by both methods. The common bias suggests an origin within the MMT fractions~~. However, ~~, although the aerosol measurements themselves are infrequent and subject to uncertainty. ~~Another possible reason for underestimate of iron oxide is that the MMTprescribes only hematite, even though goethite is also~~ The underestimation of iron oxides may also result from the exclusion of goethite from the MMT, a mineral that is a source of aerosol iron (Formenti et al., 2014a; Journet et al., 2014).

Both the SMF and AMF experiments reveal a smaller range of mineral ratios compared to the observations. This is ~~possibly~~ partly a consequence of model resolution that is insufficient to resolve strong spatial contrasts in mineral fractions ~~around~~ near isolated source regions. ~~Alternatively, large local variations in the ratio between different minerals may be reduced during construction of~~ In addition, spatial variations of soil mineral composition are reduced by the MMT that consists of ~~averages over different~~ a single average value for all examples of the same arid soil type. Common features of the AMF and SMF mineral fractions at clay sizes are a useful test of the MMT, because the emitted fractions in both experiments are unmodified by ~~our method of~~ reaggregation. Recent studies have proposed refinements to the MMT based upon a greater number of soil measurements and inclusion of additional minerals such as ~~chlorite, vermiculite and goethite that are present in measurements~~goethite, chlorite and vermiculite (Journet et al., 2014). These refinements can be complemented with studies that map the mineral composition of specific sources (Formenti et al., 2014b). However, we emphasize that there ~~are other potential sources of model error, including different removal rates resulting from variations of mineral solubility~~remain errors in our model representation of the aerosol life cycle.

~~We also suggest that several errors may originate~~ Errors may also arise from our apportionment of the emitted silt ~~minerals~~ to the transported size bins. ~~We currently use~~ The AMF method currently apportions silt emission using size-resolved measurements of ~~surface concentration of individual minerals at~~ individual minerals after transport to Tinfou, Morocco. ~~However, evaluation~~ Evaluation of the model mineral fractions suggests that prior deposition has preferentially removed the largest particles (cf. Fig. ~~18~~17 of Perlwitz et al., 2015), resulting in an underestimate of emission at the largest silt sizes. This ~~corresponds to~~

results in a compensating overestimate of emission at the smallest silt sizes ~~. This accounts for~~ (due to the normalization of the prescribed size distribution), contributing to excessive model values of PM_{10} near ~~source regions, and has~~ sources. Errors in the size distribution of emission have implications for the long-range transport of particular minerals like quartz that are typically emitted at larger sizes. This emphasizes the need for size-resolved measurements of emission that distinguish between individual minerals and can replace our current prescription based upon measurements ~~of surface concentration~~after transport.

~~Our study is complementary to that of Scanza et al. (2014), who represented brittle fragmentation and reaggregation of the wet-sieved soil to derive the mineral composition of dust aerosols. The improved evaluation of the AMF method in our study in contrast to that of the SMF experiment supports the importance of these processesthat modify the mineral fractions of the wet-sieved soil. This shows that these processes need to be included when calculating the climate impact of the individual minerals comprising dust, such as their effect as ice nuclei (Hoose et al., 2008; Atkinson et al., 2013). The improved performance of the AMF method shows that the MMT must be augmented with additional information about the original, undisturbed parent soil subject to wind erosion along with the emission process. The~~ This study is a step toward calculating the influence of aerosol mineral composition upon climate, including radiative forcing, physical and chemical transformation during transport and aerosol solubility, among other processes. While the global distribution of quartz and phyllosilicates like illite and kaolinite are probably the best characterized by measurements, other minerals with important climate impacts are subject to fewer constraints. This is especially true for minerals like montmorillonite (a member of the smectite group) and feldspar that are subject to fewer measurements, resulting in an uncertain spatial distribution despite these minerals' potential importance for ice nucleation (Hoose et al., 2008; Atkinson et al., 2013). Note that the regional distribution of ~~proposed ice nuclei like phyllosilicates~~ smectite and feldspar are very different between the SMF and AMF experiments (cf. Figs. 14 and 15 of Perlwitz et al., 2015)~~, corresponding to a large uncertainty in the impact of these minerals. The limited measurements of aerosol size (that influences global dispersal) are generally insufficient to evaluate the~~

~~model spatial distribution of the minerals serving as ice nuclei. This is especially true for minerals like feldspar. Moreover, sampling uncertainty of airborne minerals means that the measurements offer only limited guidance to future refinements of the MMT based upon soilanalysis. In short, the~~ . Iron oxides are also subject to few direct measurements, either airborne or in the soil, although their distribution could be constrained using retrievals of aerosol shortwave absorption (Koven and Fung, 2006). In general, the climate impacts of dust that depend upon ~~the~~ its specific mineral content ~~of the aerosols~~ remain highly uncertain and underconstrained.

Despite the extensive compilation of measurements presented in Table 1, the large remaining uncertainty limits our ability to suggest more precise treatments of aerosol mineral composition and its relation to the compositon of the parent soil. The abundant measurements of bulk mineral fractions far downwind of dust sources are particularly unhelpful to the extent that models can compensate for errors in soil composition through errors in the emitted size fraction. This ~~is important for the transport of iron oxides. Far from the source, crystalline forms of iron have generally been removed as a result of their greater density. The global dispersion of iron oxides is largely as accretions of small impurities upon the surface of other minerals, and is thus tied to the dispersion of these minerals that depends upon their lifetime and thus their size. This~~ shows the value of future measurements of aerosol mineral composition that are size resolved. Currently, these are rare, even though the technology exists for more routine sampling (e.g. Kandler et al., 2009). In contrast, measurements of elemental abundance are relatively ubiquitous and long records exist at stations like Izaña with relatively ~~little~~ small sampling uncertainty (Rodríguez et al., 2011). We will report on an evaluation of the AMF and SMF methods using elemental abundance and the implications for modeling aerosol mineral composition in a subsequent study (Pérez García-Pando et al., 2015).

Appendix A: Sampling uncertainty

We designed the ~~experiments and their evaluation with measurements~~ evaluation of the SMF and AMF experiments to emphasize the ~~influence of the calculated~~ differences between two methods of calculating aerosol mineral content. ~~For example, we~~ We compare mineral fractions rather than the absolute concentration of individual minerals to remove the effect of our uncertainty about the magnitude of global dust emission. Similarly, we relax the model winds toward reanalysis values so that the model mineral fractions are more strongly dependent upon the calculated fractions at emission rather than possible errors in aerosol transport.

Uncertainty of evaluation also results from sampling, including the occasional departure of the measurement duration from the monthly ~~averaging of~~ averages archived by the model. There are two general cases. In the first case, the measurements represent an average over a duration of a month or longer and can thus be compared directly with the archived model output. The measured quantity in this case is typically deposition. For this example, we calculate the ~~SD~~ standard deviation (SD) of the model, using the nine values available from the nine years simulated by each experiment. The SD allows us to estimate a distribution of possible model values that can be compared to the single measured value. That is, we are asking whether the measured value is consistent with the model distribution. This allows a consistent treatment of measurements that are both within and beyond the range of years corresponding to our experiments. The model mean and SD of the mineral fractions are fitted to a beta distribution that is commonly used to represent values that are bounded between zero and one (e.g. Freund, 1992). In the figures, we illustrate the distribution of model values with the 95 % confidence interval of the beta distribution.

In the second case, we have measurements like concentration whose duration is less than the single month used to archive model output. In most examples, we have ~~observations~~ multiple measurements from which we can estimate a time-average and standard error for comparison to the model. ~~This average is often over a month, and its uncertainty can be~~ If these measurements are confined to a single month, then we interpret the time average as an estimate of the monthly average that can be compared to the model output. The uncertainty of this average is estimated using the standard error $s_{\mathrm{E,O}}$:

$$s_{\mathrm{E,O}} = \frac{\sigma_{\mathrm{O}}}{\sqrt{N_{\mathrm{O}}}} \tag{A1}$$

where σ_{O} is the SD of the N_{O} observations. (For computational convenience, we assume that the observations are distributed normally about their mean rather than according to a beta distribution. Then, the inferred time-average of the observations is within two standard errors of the true value ninety-five percent of the time.) Here, we are essentially using the repeated observations to form a distribution of all possible values during the averaging interval, including those times when measurements were not taken. This distribution is then used to estimate the uncertainty of the mean. In the figures, this uncertainty is represented as two standard errors above and below the inferred time mean.

There are a few examples where daily measurements (or more generally, measurements over sub-monthly durations) are scattered over a much longer period. In some cases, the precise date of measurement is unknown (e.g. Engelbrecht et al., 2009). In these cases, the uncertainty of the corresponding time average is probably bounded by the annual cycle that we estimate using the SD of the measurements. Our uncertainty estimate is not particularly precise, but fortunately, there are relatively few cases of this type.

A more rare case is where we have a measurement for only a single day (e.g. Alastuey et al., 2005). Here we compare this single measurement directly to the monthly average of the model. We estimate the uncertainty of the single measurement as a monthly average by borrowing its SD from that calculated using the model. We cannot directly calculate the daily SD from model output, but we make the assumption that interannual variations in the model monthly means result solely from averaging over sub-monthly fluctuations. Then, we can estimate σ_{M}, the model SD at the time scale of the observation interval ΔT_{O} (one day, in this example) according to:

$$\sigma_{\mathrm{M}} = \sqrt{\frac{N_{\mathrm{M}}}{\Delta T_{\mathrm{O}}}}\sigma_{\mathrm{M,monthly}}, \tag{A2}$$

where $\sigma_{\mathrm{M,monthly}}$ is the interannual SD of the monthly averages, and N_{M} represents the number of days in the month corresponding to the measurement. In the figure, the uncertainty is illustrated as two SDs above and below the single observed value.

There are a number of assumptions that go into our calculation of measurement uncertainty. For example, Eq. (A1) assumes that successive measurements are not correlated. It is straightforward to replace the number of observations with an effective number if the data show that ~~autocorrelation cannot be neglected~~ successive measurements are autocorrelated (but we have neglected this possibility). In addition, the calculation of the sub-monthly SD in terms of interannual variability according to Eq. (A2) assumes that fluctuations of the mineral fractions have uniform spectral power at periods longer than the sub-monthly measurement interval. In general, our less defensible assumptions are necessitated by the sparse measurement record. This shows the urgent value of future measurements of aerosol mineral composition that are widespread and routine that would reduce the need for imprecise and heuristic characterizations of uncertainty like Eq. (A2). In any case, ~~the conclusions we draw~~ we try to draw conclusions from this study ~~are~~ based upon differences between the experiments that are qualitatively apparent and that do not rely upon intricate statistical analysis.

The Supplement related to this article is available online at doi:10.5194/acpd-0-1-2015-supplement.

Acknowledgements. We thank Paul Ginoux, Konrad Kandler, Jasper Kok, Natalie Mahowald, Sergio Rodríguez~~and Rachel Scanza~~, Rachel Scanza and Yves Balkanski for helpful conversations. This article was improved by the thoughtful comments of the reviewers. This research was supported by the National Science Foundation (ATM-01-24258), the Department of Energy (DE-SC0006713), the NASA Modeling, Analysis and Prediction Program and the Ministry of Economy and Competitiveness of Spain through the POLLINDUST (CGL2011-26259). NCEP Reanalysis winds were provided by the Physical Sciences Division at the National Oceanic and Atmospheric Administration Earth System Research Laboratory via http://www.esrl.noaa.gov/psd/. Computational resources were provided by the NASA High-End Computing (HEC) Program through the NASA Center for Climate Simulation (NCCS) at Goddard Space Flight Center.

References

Adedokum, J. A., Emofurieta, W. O., and Adedeji, O. A.: Physical, Mineralogical and Chemical Properties of Harmattan Dust at Ile-Ife, Nigeria, Theor. Appl. Climatol., 40, 161–169, doi:10.1007/BF00866179, http://dx.doi.org/10.1007/BF00866179, 1989.

Al-Awadhi, J. M. and AlShuaibi, A. A.: Dust fallout in Kuwait city: Deposition and characterization, Science of The Total Environment, 461–462, 139–148, doi:10.1016/j.scitotenv.2013.03.052, http://dx.doi.org/10.1016/j.scitotenv.2013.03.052, 2013.

Al-Dousari, A. M. and Al-Awadhi, J.: Dust fallout in Northern Kuwait, major sources and characteristics, Kuwait J. Sci., 39, 171–187, 2012.

Al-Dousari, A. M., Al-Awadhi, J., and Ahmed, M.: Dust fallout characteristics within global dust storm major trajectories, Arab. J. Geosci., 6, 3877–3884, doi:10.1007/s12517-012-0644-0, http://dx.doi.org/10.1007/s12517-012-0644-0, 2013.

Alastuey, A., Querol, X., Castillo, S., Escudero, M., Avila, A., Cuevas, E., Torres, C., Romero, P.-M., Exposito, F., García, O., Diaz, J. P., Van Dingenen, R., and Putaud, J. P.: Characterisation of TSP and PM2.5 at Izaña and Sta. Cruz de Tenerife (Canary Islands, Spain) during a Saharan Dust Episode (July 2002), Atmos. Environ., 39, 4715–4728, doi:10.1016/j.atmosenv.2005.04.018, http://dx.doi.org/10.1016/j.atmosenv.2005.04.018, 2005.

Alfaro, S. C. and Gomes, L.: Modeling mineral aerosol production by wind erosion: Emission intensities and aerosol size distributions in source areas., J. Geophys. Res., 106, 18 075–18 084, doi:10.1029/2000JD900339, http://dx.doi.org/10.1029/2000JD900339, 2001.

Arnold, E., Merrill, J., Leinen, M., and King, J.: The effect of source area and atmospheric transport on mineral aerosol collected over the North Pacific Ocean, Global and Planetary Change, 18, 137–159, doi:10.1016/S0921-8181(98)00013-7, http://dx.doi.org/10.1016/S0921-8181(98)00013-7, 1998.

Aston, S. R., Chester, R., Johnson, L. R., and Padgham, R. C.: Eolian Dust From The Lower Atmosphere Of The Eastern Atlantic And Indian Oceans, China Sea And Sea Of Japan, Marine Geology, 14, 15–28, doi:10.1016/0025-3227(73)90040-6, http://dx.doi.org/10.1016/0025-3227(73)90040-6, 1973.

Atkinson, J. D., Murray, B. J., Woodhouse, M. T., Whale, T. F., Baustian, K. J., Carslaw, K. S., Dobbie, S., O'Sullivan, D., and Malkin, T. L.: The importance of feldspar for ice nucleation by mineral dust in mixed-phase clouds, Nature, 498, 355–358, doi:10.1038/nature12278, http://dx.doi.org/10.1038/nature12278, 2013.

Avila, A., Queralt-Mitjans, I., and Alcarcón, M.: Mineralogical composition of African dust delivered by red rains over northeastern Spain, J. Geophys. Res., 102, 21 977–21 996, doi:10.1029/97JD00485, 1997.

Awadh, S. M.: Geochemistry and mineralogical composition of the airborne particles of sand dunes and dust storms settled in Iraq and their environmental impact, Environ. Earth. Sci., 66, 2247–2256, doi:10.1007/s12665-011-1445-6, http://dx.doi.org/10.1007/s12665-011-1445-6, 2012.

Baker, A. R., Laskina, O., and Grassian, V. H.: Processing and Ageing in the Atmosphere, in: Mineral Dust: A Key Player in the Earth System, edited by Knippertz, P. and Stuut, J.-B. W., chap. 4, pp. 75–92, Springer Netherlands, Dordrecht, Heidelberg, New York, London, doi:10.1007/978-94-017-8978-3_4, http://link.springer.com/chapter/10.1007%2F978-94-017-8978-3_4, 2014.

Bauer, S. E. and Koch, D.: Impact of heterogeneous sulfate formation at mineral dust surfaces on aerosol loads and radiative forcing in the Goddard Institute for Space Studies general circulation model, J. Geophys. Res., 110, D17202, doi:10.1029/2005JD005870, http://dx.doi.org/10.1029/2005JD005870, 2005.

Cakmur, R. V., Miller, R. L., and Torres, O.: Incorporating the effect of small-scale circulations upon dust emission in an atmospheric general circulation model, J. Geophys. Res., 109, D07201, doi:10.1029/2003JD004067, http://dx.doi.org/10.1029/2003JD004067, 2004.

Caquineau, S., Gaudichet, A., Gomes, L., Magonthier, M., and Chatenet, B.: Saharan dust: Clay ratio as a relevant tracer to assess the origin of soil-derived aerosols, Geophys. Res. Lett., 25, 983–986, doi:10.1029/98GL00569, http://dx.doi.org/10.1029/98GL00569, 1998.

Chester, R. and Johnson, L. R.: Atmospheric Dusts Collected off the Atlantic Coast of North Africa and the Iberian Peninsula, Marine Geology, 11, 251–260, doi:10.1016/0025-3227(71)90027-2, http://dx.doi.org/10.1016/0025-3227(71)90027-2, 1971a.

Chester, R. and Johnson, L. R.: Atmospheric Dust Collected Off the West African Coast, Nature, 229, 105–107, doi:10.1038/229105b0, http://dx.doi.org/10.1038/229105b0, 1971b.

Chester, R., Elderfield, H., and Griffin, J. J.: Dust transported in the North-east and South-east Trade Winds in the Atlantic Ocean, Nature, 233, 474–476, doi:10.1038/233474a0, http://dx.doi.org/10.1038/233474a0, 1971.

Chester, R., Elderfield, H., Griffin, J. J., Johnson, L., and Padgham, R. C.: Eolian dust along the eastern margins of the Atlantic Ocean, Marine Geology, 13, 91–105, doi:10.1016/0025-3227(72)90048-5, http://dx.doi.org/10.1016/0025-3227(72)90048-5, 1972.

Chester, R., Baxter, G. G., Behairy, A. K. A., Connor, K., Cross, D., Elderfield, H., and Padgham, R. C.: Soil-sized eolian dusts from the lower troposphere of the eastern Mediterranean Sea, Marine Geology, 24, 201–217, doi:10.1016/0025-3227(77)90028-7, http://dx.doi.org/10.1016/0025-3227(77)90028-7, 1977.

Chester, R., Sharples, E. J., Sanders, G. S., and Saydam, A. C.: Saharan Dust Incursion Over The Tyrrhenian Sea, Atmos. Environ., 18, 929–935, doi:10.1016/0004-6981(84)90069-6, http://dx.doi.org/10.1016/0004-6981(84)90069-6, 1984.

Choate, L. M., Ranville, J. F., Bunge, A. L., and Macalady, D. L.: Dermally adhered soil: 2. Reconstruction of dry-sieve particle-size distributions from wet-sieve data, Integrated Environmental Assessment and Management, 2, 385–390, doi:10.1002/ieam.5630020410, http://dx.doi.org/10.1002/ieam.5630020410, 2006.

Claquin, T., Schulz, M., and Balkanski, Y. J.: Modeling the mineralogy of atmospheric dust sources, J. Geophys. Res., 104, 22,243–22,256, doi:10.1029/1999JD900416, http://dx.doi.org/10.1029/1999JD900416, 1999.

Delany, A. C., Delany, A. C., Parkin, D. W., Griffin, J. J., Goldberg, E. D., and Reimann, B. E. F.: Airborne dust collected at Barbados, Geochimica et Cosmochimica Acta, 31, 885–909, doi:10.1016/S0016-7037(67)80037-1, http://dx.doi.org/10.1016/S0016-7037(67)80037-1, 1967.

Díaz-Hernández, J. L., Martín-Ramos, J. D., and Lṕez-Galindo, A.: Quantitative analysis of mineral phases in atmospheric dust deposited in the south-eastern Iberian Peninsula, Atmos. Environ., 45, 3015–3024, doi:10.1016/j.atmosenv.2011.03.024, http://dx.doi.org/10.1016/j.atmosenv.2011.03.024, 2011.

Enete, I. C., Obienusi, E. A., Igu, I. N., and Ayadiulo, R.: Harmattan Dust: Composition, Characteristics and Effects on Soil Fertility in Enugu, Nigeria, British Journal of Applied Science & Technology, 2, 72–81, doi:10.9734/BJAST/2012/950, http://dx.doi.org/10.9734/BJAST/2012/950, 2012.

Engelbrecht, J. P., McDonald, E. V., Gillies, J. A., Jayanty, R. K. M., Casuccio, G., and Gertler, A. W.: Characterizing Mineral Dusts and Other Aerosols from the Middle East — Part 1: Ambient Sampling, Inhalation Toxicology, 21, 297–326, doi:10.1080/08958370802464273, http://dx.doi.org/10.1080/08958370802464273, 2009.

Engelbrecht, J. P., Menéndez, I., and Derbyshire, E.: Sources of $PM_{2.5}$ impacting on Gran Canaria, Spain, CATENA, 117, 119–132, doi:10.1016/j.catena.2013.06.017, http://dx.doi.org/10.1016/j.catena.2013.06.017, 2014.

Falkovich, A. H., Ganor, E., Levin, Z., Formenti, P., and Rudich, Y.: Chemical and mineralogical analysis of individual mineral dust particles, J. Geophys. Res., 106, 18,029–18,036, doi:10.1029/2000JD900430, http://dx.doi.org/10.1029/2000JD900430, 2001.

FAO: Digital Soil Map of the World and Derived Soil Properties, Food and Agriculture Organization, Rome, Italy, 1995.

FAO: Digital Soil Map of the World, Food and Agriculture Organization, Rome, Italy, 2007.

FAO/IIASA/ISRIC/ISSCAS/JRC: Harmonized World Soil Database (version 1.2), FAO, Rome, Italy and IIASA, Laxenburg, Austria, http://webarchive.iiasa.ac.at/Research/LUC/External-World-soil-database/HTML/HWSD_Data.html?sb=4, last access date: 24 January 2013, 2012.

Ferguson, W. S., Griffin, J. J., and Goldberg, E. D.: Atmospheric Dust from the North Pacific – A short note on a long range eolian transport, J. Geophys. Res., 75, 1137–1139, doi:10.1029/JC075i006p01137, http://dx.doi.org/10.1029/JC075i006p01137, 1970.

Fiol, L. A., Fornós, J. J., Gelabert, B., and Guijarro, J. A.: Dust rains in Mallorca (Western Mediterranean): Their occurrence and role in some recent geological processes, Catena, 63, 64–84, doi:10.1016/j.catena.2005.06.012, http://dx.doi.org/10.1016/j.catena.2005.06.012, 2005.

Formenti, P., Rajot, J. L., Desboeufs, K., Caquineau, S., Chevaillier, S., Nava, S., Gaudichet, A., Journet, E., Triquet, S., Alfaro, S., Chiari, M., Haywood, J., Coe, H., , and Highwood, E.: Regional variability of the composition of mineral dust from western Africa: Results from the AMMA SOP0/DABEX and DODO field campaigns, J. Geophys. Res., 113, D00C13, doi:10.1029/2008JD009903, http://dx.doi.org/10.1029/2008JD009903, 2008.

Formenti, P., Caquineau, S., Chevaillier, S., Klaver, A., Desboeufs, K., Rajot, J. L., Belin, S., and Briois, V.: Dominance of goethite over hematite in iron oxides of mineral dust from Western Africa:

Quantitative partitioning by X-ray absorption spectroscopy, J. Geophys. Res., Early View, 15 pgs., doi:10.1002/2014JD021668, http://dx.doi.org/10.1002/2014JD021668, 2014a.

Formenti, P., Caquineau, S., Desboeufs, K., Klaver, A., Chevaillier, S., Journet, E., and Rajot, J. L.: Mapping the physico-chemical properties of mineral dust in western Africa: mineralogical composition, Atmos. Chem. Phys., 14, 10 663–10 686, doi:10.5194/acp-14-10663-2014, http://dx.doi.org/10.5194/acp-14-10663-2014, 2014b.

Freund, J. E.: Mathematical Statistics, Prentice Hall, Inc., Englewood Cliffs, New Jersey, 5th edn., 1992.

Frinak, E. K., Mashburn, C. D., Tolbert, M. A., and Toon, O. B.: Infrared characterization of water uptake by low-temperature Na-montmorillonite: Implications for Earth and Mars, J. Geophys. Res., 110, D09308, doi:10.1029/2004JD005647, http://dx.doi.org/10.1029/2004JD005647, 2005.

Game, P. M.: Observations on a dustfall in the Eastern Atlantic, February, 1962, Journal of Sedimentary Petrology, 34, 355–359, doi:10.1306/74D7105F-2B21-11D7-8648000102C1865D, http://jsedres.geoscienceworld.org/content/34/2/355.abstract, 1964.

Ganor, E.: The composition of clay minerals transported to Israel as indicators of Saharan dust emission, Atmospheric Environment, 25, 2657–2664, doi:10.1016/0960-1686(91)90195-D, http://dx.doi.org/10.1016/0960-1686(91)90195-D, 1991.

Ganor, E., Deutsch, Y., and Foner, H. A.: Mineralogical Composition and Sources of Airborne Settling Particles on Lake Kinneret (the Sea of Galilee), Israel, Water, Air, and Soil Pollution, 118, 245–262, doi:10.1023/A:1005167230795, http://dx.doi.org/10.1023/A:1005167230795, 2000.

Gao, Y. and Anderson, J. R.: Characteristics of Chinese aerosols determined by individual-particle analysis, J. Geophys. Res., 106, 18 037–18 045, doi:10.1029/2000JD900725, http://dx.doi.org/10.1029/2000JD900725, 2001.

Gaudichet, A., Lefèvre, R., Gaudry, A., Ardouin, B., Lambert, G., and Miller, J. M.: Mineralogical composition of aerosols at Amsterdam Island, Tellus, 41, 344–352, doi:10.1111/j.1600-0889.1989.tb00313.x, http://dx.doi.org/10.1111/j.1600-0889.1989.tb00313.x, 1989.

Gaudichet, A., Angclis, M. D., Joussaume, S., Petit, J. R., Korotkevitch, Y. S., and Petrov, V. N.: Comments on the origin of dust in East Antarctica for present and ice-age conditions, J. Atmos. Chem., 14, 192–142, doi:10.1007/BF00115229, http://dx.doi.org/10.1007/BF00115229, 1992.

~~Gillette, D. A., Blifford JR., I. H., and Fryrear, D. W.: The Influence of Wind Velocity on the Size Distributions of Aerosols Generated by the Wind Erosion of Soils, J. Geophys. Res., 79, 4068–4075, doi:10.1029/JC079i027p04068, http://dx.doi.org/10.1029/JC079i027p04068, 1974.~~

Ginoux, P., Chin, M., Tegen, I., Prospero, J. M., Holben, B., Dubovik, O., and Lin, S.-J.: Sources and distributions of dust aerosols simulated with the GOCART model, J. Geophys. Res., 106, 20,255–20,273, doi:10.1029/2000JD000053, http://dx.doi.org/10.1029/2000JD000053, 2001.

Glaccum, R. A. and Prospero, J. M.: Saharan aerosols over the tropical North Atlantic – Mineralogy, Marine Geology, 37, 295–321, doi:10.1016/0025-3227(80)90107-3, http://dx.doi.org/10.1016/0025-3227(80)90107-3, 1980.

Goldberg, E. D. and Griffin, J. J.: The sediments of the Northern Indian Ocean, Deep Sea Res., 17, 513–537, doi:10.1016/0011-7471(70)90065-3, http://dx.doi.org/10.1016/0011-7471(70)90065-3, 1970.

Grini, A., Zender, C. S., and Colarco, P. R.: Saltation Sandblasting behavior during mineral dust aerosol production, Geophys. Res. Lett, 29, 1868, doi:10.1029/2002GL015248, http://dx.doi.org/10.1029/2002GL015248, 2002.

Hoose, C., Lohmann, U., Erdin, R., and Tegen, I.: The global influence of dust mineralogical composition on heterogeneous ice nucleation in mixed-phase clouds, Environ. Res. Lett., 3, 14 pp, doi:10.1088/1748-9326/3/2/025003, http://iopscience.iop.org/1748-9326/3/2/025003/, 2008.

Iversen, J. D. and White, B. R.: Saltation threshold on Earth, Mars and Venus, Sedimentology, 29, 111–119, doi:10.1111/j.1365-3091.1982.tb01713.x, http://dx.doi.org/10.1111/j.1365-3091.1982.tb01713.x, 1982.

Jeong, G. Y.: Bulk and single-particle mineralogy of Asian dust and a comparison with its source soils, J. Geophys. Res., 113, D02208, doi:10.1029/2007JD008606, http://dx.doi.org/10.1029/2007JD008606, 2008.

Jeong, G. Y. and Achterberg, E. P.: Chemistry and mineralogy of clay minerals in Asian and Saharan dusts and the implications for iron availability, Atmos. Chem. Phys. Discuss., 14, 15 735–15 770, doi:10.5194/acpd-14-15735-2014, http://dx.doi.org/10.5194/acpd-14-15735-2014, 2014.

Jeong, G. Y., Kim, J. Y., Seo, J., Kim, G. M., Jin, H. C., and Chun, Y.: Long-range transport of giant particles in Asian dust identified by physical, mineralogical, and meteorological analysis, Atmos. Chem. Phys., 14, 505–521, doi:10.5194/acp-14-505-2014, http://dx.doi.org/10.5194/acp-14-505-2014, 2014.

Johnson, L. R.: Particle-Size Fractionation of Eolian Dust During Transport and Sampling, Marine Geology, 21, M17–M21, doi:10.1016/0025-3227(76)90099-2, http://dx.doi.org/10.1016/0025-3227(76)90099-2, 1976.

Journet, E., Balkanski, Y., and Harrison, S. P.: A new data set of soil mineralogy for dust-cycle modeling, Atmos. Chem. Phys., 14, 3801–3816, doi:10.5194/acp-14-3801-2014, http://dx.doi.org/10.5194/acp-14-3801-2014, 2014.

Kalnay, E., Kanamitsu, M., Kistler, R., Collins, W., Deaven, D., Gandin, L., Iredell, M., Saha, S., White, G., Woollen, J., Zhu, Y., Leetmaa, A., Reynolds, R., Chelliah, M., Ebisuzaki, W., Higgins, W., Janowiak, J., Mo, K. C., Ropelewski, C., Wang, J., Jenne, R., and Joseph, D.: The NCEP/NCAR 40-Year Reanalysis Project, Bull. Amer. Meteor. Soc., 77, 437–471, doi:10.1175/1520-0477(1996)077<0437:TNYRP>2.0.CO;2, http://journals.ametsoc.org/doi/abs/10.1175/1520-0477%281996%29077%3C0437%3ATNYRP%3E2.0.CO%3B2, 1996.

Kandler, K., Benker, N., Bundke, U., Cuevas, E., Ebert, M., Knippertz, P., Rodríguez, S., Schütz, L., and Weinbruch, S.: Chemical composition and complex refractive index of Saharan Mineral Dust at Izanã, Tenerife (Spain) derived by electron microscopy, Atmospheric Environment, 41, 8058–8074, doi:10.1016/j.atmosenv.2007.06.047, http://dx.doi.org/10.1016/j.atmosenv.2007.06.047, 2007.

Kandler, K., Schütz, L., Deutscher, C., Ebert, M., Hofmann, H., Jäckel, S., Jaenicke, R., Knippertz, P., Lieke, K., Massling, A., Petzold, A., Schladitz, A., Weinzierl, B., Wiedensohler, A., Zorn, S., and Weinbruch, S.: Size distribution, mass concentration, chemical and mineralogical composition and derived optical parameters of the boundary layer aerosol at Tinfou, Morocco, during SAMUM 2006, Tellus B, 61, 32–50, doi:10.1111/j.1600-0889.2008.00385.x, http://dx.doi.org/10.1111/j.1600-0889.2008.00385.x, 2009.

Kandler, K., Schütz, L., Jäckel, S., Lieke, K., Emmel, C., Müller-Ebert, D., Ebert, M., Scheuvens, D., Schladitz, A., Šegvić, B., Wiedensohler, A., and Weinbruch, S.: Ground-based off-line aerosol measurements at Praia, Cape Verde, during the Saharan Mineral Dust Experiment: microphysical properties and mineralogy, Tellus B, 63, 459–474, doi:10.1111/j.1600-0889.2011.00550.x, http://dx.doi.org/10.1111/j.1600-0889.2011.00550.x, 2011.

Khalaf, F. I., Al-Kadi, A., and Al-Saleh, S.: Mineralogical composition and potential sources of dust fallout deposits in Kuwait, northern Arabian Gulf, Sedimentary Geology, 42, 255–278, doi:10.1016/0037-0738(85)90047-8, http://dx.doi.org/10.1016/0037-0738(85)90047-8, 1985.

Klaver, A., Formenti, P., Caquineau, S., Chevaillier, S., Ausset, P., Calzolai, G., Osborne, S., Johnson, B., Harrison, M., and Dubovik, O.: Physico-chemical and optical properties of Sahelian and Saharan mineral dust: in situ measurements during the GERBILS campaign, Q. J. Roy. Meteor. Soc., 137, 1193–1210, doi:10.1002/qj.889, http://dx.doi.org/10.1002/qj.889, 2011.

Koch, D., Jacob, D., Tegen, I., Rind, D., and Chin, M.: Tropospheric sulfur simulation and sulfate direct radiative forcing in the Goddard Institute for Space Studies general circulation model, J. Geophys. Res., 104, 23,799–23,822, doi:10.1029/1999JD900248, http://dx.doi.org/10.1029/1999JD900248, 1999.

Kok, J. F.: A scaling theory for the size distribution of emitted dust aerosols suggests climate models underestimate the size of the global dust cycle, PNAS, 108, 1016–1021, doi:10.1073/pnas.1014798108, http://www.pnas.org/content/108/3/1016, 2011.

Koven, C. D. and Fung, I.: Inferring dust composition from wavelength-dependent absorption in Aerosol Robotic Network (AERONET) data, J. Geophys. Res., 111, D14205, doi:10.1029/2005JD006678, http://dx.doi.org/10.1029/2005JD006678, 2006.

Lafon, S., Sokolik, I. N., Rajot, J. L., Caquineau, S., and Gaudichet, A.: Characterization of iron oxides in mineral dust aerosols: Implications for light absorption, J. Geophys. Res., 111, D21207, doi:10.1029/2005JD007016, http://dx.doi.org/10.1029/2005JD007016, 2006.

Laurent, B., Marticorena, B., Bergametti, G., Léon, J. F., and Mahowald, N. M.: Modeling mineral dust emissions from the Sahara desert using new surface properties and soil database, Journal of Geophysical Research: Atmospheres (1984–2012), 113, D14218, doi:10.1029/2007JD009484, http://dx.doi.org/10.1029/2007JD009484, 2008.

Leinen, M., Prospero, J. M., Arnold, E., and Blank, M.: Mineralogy of aeolian dust reaching the North Pacific Ocean 1. Sampling and analysis, J. Geophys. Res., 99, 21,017–21,023, doi:10.1029/94JD01735, http://dx.doi.org/10.1029/94JD01735, 1994.

Lu, S., Shao, L., Wu, M., and Jiao, Z.: Mineralogical characterization of airborne individual particulates in Bejing PM_{10}, J. Environ. Sci., 18, 90–95, http://iospress.metapress.com/content/52ganfy7xb25a0ma/, 2006.

McFadden, L. D. and Hendricks, D. M.: Changes in the content and composition of pedogenic iron oxyhydroxides in a chronosequence of soils in southern California, Quaternary Research, 23, 189–204, doi:10.1016/0033-5894(85)90028-6, http://dx.doi.org/10.1016/0033-5894(85)90028-6, 1985.

Menéndez, I., Díaz-Hernández, J. L., Mangas, J., Alonso, I., and Sánchez-Soto, P. J.: Airborne dust accumulation and soil development in the North-East sector of Gran Canaria (Canary Islands, Spain), J. Arid Environ., 71, 57–81, doi:10.1016/j.jaridenv.2007.03.011, http://dx.doi.org/10.1016/j.jaridenv.2007.03.011, 2007.

Miller, R. L., Cakmur, R. V., Perlwitz, J., Geogdzhayev, I. V., Ginoux, P., Koch, D., Kohfeld, K. E., Prigent, C., Ruedy, R., Schmidt, G. A., and Tegen, I.: Mineral dust aerosols in the NASA Goddard

Institute for Space Sciences ModelE atmospheric general circulation model, J. Geophys. Res., 111, D06208, doi:10.1029/2005JD005796, http://dx.doi.org/10.1029/2005JD005796, 2006.

Møberg, J. P., Esu, I. E., and Malgwi, W. B.: Characteristics and constituent composition of Harmattan dust falling in Northern Nigeria, Geoderma, 48, 73–81, doi:10.1016/0016-7061(91)90007-G, http://dx.doi.org/10.1016/0016-7061(91)90007-G, 1991.

Moulin, C., Lambert, C. E., Dulac, F., and Dayan, U.: Control of atmospheric export of dust from North Africa by the North Atlantic Oscillation, Nature, 387, 691–694, http://www.nature.com/nature/journal/v387/n6634/full/387691a0.html, 1997.

Navea, J. G., Chen, H., Huang, M., Carmichael, G. R., and Grassian, V. H.: A comparative evaluation of water uptake on several mineral dust sources, Environ. Chem., 7, 162–170, doi:10.1071/EN09122, http://www.publish.csiro.au/?paper=EN09122, 2010.

Nickovic, S., Vukovic, A., Vujadinovic, M., Djurdjevic, V., and Pejanovic, G.: Technical Note: High-resolution mineralogical database of dust-productive soils for atmospheric dust modeling, Atmos. Chem. Phys., 12, 845–855, doi:10.5194/acp-12-845-2012, http://dx.doi.org/10.5194/acp-12-845-2012, 2012.

NRCS Soil Survey Staff: U.S. General Soil Map (STATSGO), Natural Resources Conservation Service, United States Department of Agriculture, http://sdmdataaccess.nrcs.usda.gov/, last access date: 11 April 2013, 2012.

O'Hara, S. L., Clarke, M. L., and Elatrash, M. S.: Field measurements of desert dust deposition in Libya, Atmos. Environ., 40, 3881–3897, doi:10.1016/j.atmosenv.2006.02.020, http://dx.doi.org/10.1016/j.atmosenv.2006.02.020, 2006.

Parkin, D. W., Phillips, D. R., Sullivan, R. A. L., and Johnson, L.: Airborne dust collections over the North Atlantic, J. Geophys. Res., 75, 1782–1793, doi:10.1029/JC075i009p01782, http://dx.doi.org/10.1029/JC075i009p01782, 1970.

Parkin, D. W., Phillips, D. R., Sullivan, R., and Johnson, L.: Airborne dust collections down the Atlantic, Quarterly Journal of the Royal Meteorological Society, 98, 798–808, doi:10.1002/qj.49709841807, http://dx.doi.org/10.1002/qj.49709841807, 1972.

Pérez García-Pando, C., Perlwitz, J. P., Miller, R. L., and Rodriguez, S.: Predicting the mineral composition of dust aerosols: Insights from elemental composition measurements at the Izaña Observatory, Geophys. Res. Lett., (in preparation), 2015.

Perlwitz, J. P., Pérez García-Pando, C., and Miller, R. L.: Predicting the mineral composition of dust aerosols. Part I: Representing key processes, Atmos. Chem. Phys. Discuss., 15, 3493–

3575, doi:10.5194/acpd-15-3493-2015, http://www.atmos-chem-phys-discuss.net/15/3493/2015/acpd-15-3493-2015.html, 2015.

Prigent, C., Tegen, I., Aires, F., Marticorena, B., and Zribi, M.: Estimation of the aerodynamic roughness length in arid and semi-arid regions over the globe with the ERS scatterometer, J. Geophys. Res., 110, D09205, doi:10.1029/2004JD005370, http://dx.doi.org/10.1029/2004JD005370, 2005.

Prospero, J. M. and Bonatti, E.: Continental Dust in the Atmosphere of the Eastern Equatorial Pacific, J. Geophys. Res., 74, 3362–3371, doi:10.1029/JC074i013p03362, http://dx.doi.org/10.1029/JC074i013p03362, 1969.

Prospero, J. M., Glaccum, R. A., and Nees, R. T.: Atmospheric transport of soil dust from Africa to South America, Nature, 289, 570–572, doi:10.1038/289570a0, http://dx.doi.org/10.1038/289570a0, 1981.

Prospero, J. M., Ginoux, P., Torres, O., Nicholson, S. E., and Gill, T. E.: Environmental characterization of global sources of atmospheric soil dust identified with the Nimbus 7 Total Ozone Mapping Spectrometer (TOMS) absorbing aerosol product, Rev. Geophys., 40, 2–1–2–31, doi:10.1029/2000RG000095, http://dx.doi.org/10.1029/2000RG000095, 2002.

Queralt-Mitjans, I., Domingo, F., and Sole-Benet, A.: The influence of local sources on the mineral content of bulk deposition over an altitudinal gradient in the Filabres Range (SE Spain), J. Geop, 98, 16,761–16,768, doi:10.1029/93JD01281, http://dx.doi.org/10.1029/93JD01281, 1993.

Rashki, A., Eriksson, P. G., de W. Rautenbach, C. J., Kaskaoutis, D. G., Grote, W., and Dykstra, J.: Assessment of chemical and mineralogical characteristics of airborne dust in the Sistan region, Iran, Chemosphere, 90, 227–236, doi:10.1016/j.chemosphere.2012.06.059, http://dx.doi.org/10.1016/j.chemosphere.2012.06.059, 2013.

Rayner, N. A., Parker, D. E., Horton, E. B., Folland, C. K., Alexander, L. V., Rowell, D. P., Kent, E. C., and Kaplan, A.: Global analyses of sea surface temperature, sea ice, and night marine air temperature since the late nineteenth century, J. Geophys. Res., 108, 4407, doi:10.1029/2002JD002670, http://dx.doi.org/10.1029/2002JD002670, 2003.

Rodríguez, S., Alastuey, A., Alonso-Pérez, S., Querol, X., Cuevas, E., Abreu-Afonso, J., Viana, M., Pérez, N., Pandolfi, M., and de la Rosa, J.: Transport of desert dust mixed with North African industrial pollutants in the subtropical Saharan Air Layer, Atmos. Chem. Phys., 11, 6,663–6,685, doi:10.5194/acp-11-6663-2011, http://www.atmos-chem-phys.net/11/6663/2011/acp-11-6663-2011.html, 2011.

Scanza, R. A., Mahowald, N., Ghan, S., Zender, C. S., Kok, J. F., Liu, X., and Zhang, Y.: Modeling dust as component minerals in the Community Atmosphere Model: development of framework and impact on radiative forcing, Atmos. Chem. Phys. Discuss., 14, 17 749–17 816, doi:10.5194/acpd-14-17749-2014, http://dx.doi.org/10.5194/acpd-14-17749-2014, 2014.

Scanza, R. A., Mahowald, N., Ghan, S., Zender, C. S., Kok, J. F., Liu, X., Zhang, Y., and Albani, S.: Modeling dust as component minerals in the Community Atmosphere Model: development of framework and impact on radiative forcing, Atmos. Chem. Phys, 15, 537–561, doi:10.5194/acp-15-537-2015, http://www.atmos-chem-phys.net/15/537/2015/acp-15-537-2015.html, 2015.

Scheuvens, D. and Kandler, K.: On Composition, Morphology, and Size Distribution of Airborne Mineral Dust, in: Mineral Dust: A Key Player in the Earth System, edited by Knippertz, P. and Stuut, J.-B., chap. 2, pp. 15–49, Springer Netherlands, Dordrecht, Heidelberg, New York, London, doi:10.1007/978-94-017-8978-3_2, http://dx.doi.org/10.1007/978-94-017-8978-3_2, 2014.

Scheuvens, D., Schütz, L., Kandler, K., Ebert, M., and Weinbruch, S.: Bulk composition of northern African dust and its source sediments and its source sediments - A compilation, Earth-Science Reviews, 116, 170–194, doi:10.1016/j.earscirev.2012.08.005, http://dx.doi.org/10.1016/j.earscirev.2012.08.005, 2013.

Schmidt, G. A., Ruedy, R., Hansen, J. E., Aleinov, I., Bell, N., Bauer, M., Bauer, S., Cairns, B., Canuto, V., Ye Cheng, A. D., Faluvegi, G., Friend, A. D., Hall, T. M., Hu, Y., Kelley, M., Kiang, N. Y., Koch, D., Andy A. Lacis, J. L., Lo, K. K., Miller, R. L., Nazarenko, L., Oinas, V., Perlwitz, J., Rind, J. P. D., Romanou, A., Gary L. Russell, M. S., Shindell, D. T., Stone, P. H., Sun, S., Tausnev, N., Thresher, D., , and Yao, M.-S.: Present-Day Atmospheric Simulations Using GISS ModelE: Comparison to In Situ, Satellite, and Reanalysis Data, J. Climate, 19, 153–192, doi:10.1175/JCLI3612.1, http://dx.doi.org/10.1175/JCLI3612.1, 2006.

Schmidt, G. A., Kelley, M., Nazarenko, L., Ruedy, R., Russell, G. L., Aleinov, I., Bauer, M., Bauer, S. E., Bhat, M. K., Bleck, R., Canuto, V., Chen, Y.-H., Cheng, Y., Clune, T. L., Del Genio, A., de Fainchtein, R., Faluvegi, G., Hansen, J. E., Healy, R. J., Kiang, N. Y., Koch, D., Lacis, A. A., LeGrande, A. N., Lerner, J., Lo, K. K., Matthews, E. E., Menon, S., Miller, R. L., Oinas, V., Oloso, A. O., Perlwitz, J. P., Puma, M. J., Putman, W. M., Rind, D., Romanou, A., Sato, M., Shindell, D. T., Sun, S., Syed, R. A., Tausnev, N., Tsigaridis, K., Unger, N., Voulgarakis, A., Yao, M.-S., and Zhang, J.: Configuration and assessment of the GISS ModelE2 contributions to the CMIP5 archive, J. Adv. Model. Earth Sys., 6, 141–184, doi:10.1002/2013MS000265, http://dx.doi.org/10.1002/2013MS000265, 2014.

Shao, L., Li, W., Xiao, Z., and Sun, Z.: The mineralogy and possible sources of spring dust particles over Bejing, Adv. Atmos. Sci., 25, 395–403, doi:10.1007/s00376-008-0395-8, http://dx.doi.org/10.1007/s00376-008-0395-8, 2008.

Shao, Y.: A model for mineral dust emission, J. Geophys. Res., 106, 20 239–20 254, doi:10.1029/2001JD900171, http://dx.doi.org/10.1029/2001JD900171, 2001.

Shao, Y., Raupach, M. R., and Leys, J. F.: A model for predicting aeolian sand drift and dust entrainment on scales from paddock to region, Aust. J. Soil Res., 34, 309–342, doi:10.1071/SR9960309, http://dx.doi.org/10.1071/SR9960309, 1996.

Shen, Z., Cao, J., Li, X., Okuda, T., Wang, Y., and Wang, X.: Mass concentration and mineralogical characteristics of aerosol particles collected at Dunhuang during ACE-Asia, Adv. Atmos. Sci., 23, 291–298, doi:10.1007/s00376-006-0291-z, http://dx.doi.org/10.1007/s00376-006-0291-z, 2006.

Shen, Z., Caquineau, S., Cao, J., Zhang, X., Han, Y., Gaudichet, A., and Gomes, L.: Mineralogical characteristics of soil dust from source regions in northern China, Particuology, 7, 507–512, doi:10.1016/j.partic.2009.10.001, http://dx.doi.org/10.1016/j.partic.2009.10.001, 2009.

Shi, Z., Shao, L., Jones, T. P., and Lu, S.: Microscopy and mineralogy of airborne particles collected during severe dust storm episodes in Beijing, China, J. Geophys. Res., 110, D01303, doi:10.1029/2004JD005073, http://dx.doi.org/10.1029/2004JD005073, 2005.

Shi, Z., Krom, M. D., Bonneville, S., Baker, A. R., Bristow, C., Drake, N., Mann, G., Carslaw, K., McQuaid, J. B., Jickells, T., and Benning, L. G.: Influence of chemical weathering and aging of iron oxides on the potential iron solubility of Saharan dust during simulated atmospheric processing, Global Biogeochem. Cycles, 25, GB2010, doi:10.1029/2010GB003837, http://dx.doi.org/10.1029/2010GB003837, 2011.

Shi, Z., Krom, M. D., Jickells, T. D., Bonneville, S., Carslaw, K. S., Mihalopoulos, N., Baker, A. R., and Benning, L. G.: Impacts on iron solubility in the mineral dust by processes in the source region and the atmosphere: A review, Aeolian Research, 5, 21–42, doi:10.1016/j.aeolia.2012.03.001, http://dx.doi.org/10.1016/j.aeolia.2012.03.001, 2012.

~~Singer, A., Dultz, S., and Argaman, E.: Properties of the non-soluble fractions of suspended dust over the Dead Sea, Atmospheric Environment, 38, 1745–1753, doi:10.1016/j.atmosenv.2003.12.026, http://dx.doi.org/10.1016/j.atmosenv.2003.12.026, 2004.~~

Skonieczny, C., Bory, A., Bout-Roumazeilles, V., Abouchami, W., Galer, S. J. G., Crosta, X., Stuut, J., Meyer, I., Chiapello, I., Podvin, T., Chatenet, B., Diallo, A., and Ndiaye, T.: The 713 March 2006 major Saharan outbreak: Multiproxy characterization of mineral dust deposited on the West

African margin, J. Geophys. Res., 116, D18210, doi:10.1029/2011JD016173, http://dx.doi.org/10.1029/2011JD016173, 2011.

Skonieczny, C., Bory, A., Bout-Roumazeilles, V., Abouchami, W., Galer, S. J. G., Crosta, X., Diallo, A., and Ndiaye, T.: A three-year time series of mineral dust deposits on the West African margin: Sedimentological and geochemical signatures and implications for interpretation of marine paleo-dust records, Earth and Planetary Science Letters, 364, 145–156, doi:10.1016/j.epsl.2012.12.039, http://dx.doi.org/10.1016/j.epsl.2012.12.039, 2013.

~~Sow, M., Alfaro, S. C., Rajot, J. L., and Marticorena, B.: Size resolved dust emission fluxes measured in Niger during 3 dust storms of the AMMA experiment, Atmos. Chem. Phys., 9, 3881–3891, doi:10.5194/acp-9-3881-2009, http://dx.doi.org/10.5194/acp-9-3881-2009, 2009.~~

Środoń, J.: Nature of mixed-layer clays and mechanisms of their formation and alteration, Annu. Rev. Earth Planet. Sci., 27, 19–53, doi:10.1146/annurev.earth.27.1.19, http://dx.doi.org/10.1146/annurev.earth.27.1.19, 1999.

Tegen, I. and Fung, I.: Modeling of mineral dust in the atmosphere: Sources, transport, and optical thickness, J. Geophys. Res., 99, 22,897–22,914, doi:10.1029/94JD01928, http://dx.doi.org/10.1029/94JD01928, 1994.

Tomadin, L., Lenaz, R., Landuzzi, V., Mazzucotelli, A., and Vannucci, R.: Wind-blown dust over the Central Mediterranean, Oceanologica Acta, 7, 13–23, 1984.

Wesely, M. L. and Hicks, B. B.: Some factors that affect the deposition rates of sulfur dioxide and similar gases on vegetation, J. Air Pollut. Control Assoc., 27, 1110–1116, doi:10.1080/00022470.1977.10470534, http://dx.doi.org/10.1080/00022470.1977.10470534, 1977.

Windom, H. L.: Atmospheric Dust Records in Permanent Snowfields: Implications to Marine Sedimentation, Geol. Soc. Amer. Bull., 80, 761–782, doi:10.1130/0016-7606(1969)80[761:ADRIPS]2.0.CO;2, http://dx.doi.org/10.1130/0016-7606(1969)80[761:ADRIPS]2.0.CO;2, 1969.

Zdanowicz, C., Hall, G., Vaive, J., Amelin, Y., Percival, J., Girard, I., Biscaye, P., and Bory, A.: Asian dustfall in the St. Elias Mountains, Yukon, Canada, Geochimica et Cosmochimica Acta, 70, 3493–3507, doi:10.1016/j.gca.2006.05.005, http://dx.doi.org/10.1016/j.gca.2006.05.005, 2006.

Zhou, G. and Tazaki, K.: Seasonal variation of gypsum in aerosol and its effect on the acidity of wet precipitation on the Japan Sea side of Japan, Atmospheric Environment, 30, 3301–3308, doi:10.1016/1352-2310(96)00071-4, http://dx.doi.org/10.1016/1352-2310(96)00071-4, 1996.

Table 1. List of literature references for mineral fraction measurements (predicted with ~~ModelE~~ModelE2: M – mica/illite/muscovite, K – kaolinite, S – smectite, C – carbonates, Q – quartz, F – feldspar, I – iron oxides, G – gypsum; not predicted other minerals: O) with specific information about months of measurements with size range, geographical coordinates, and time range of measurements.

Reference	Minerals	Size Range	Location	Time Range
Adedokum et al. (1989)	M K Q F O	Total	Ile-Ife, Nigeria	01–02/1984, 01–02/1985
Alastuey et al. (2005)	M K C Q F G O	Total	Izaña and Sta. Cruz de Tenerife, Canary Islands, Spain	07/29/2002
Al-Awadhi and AlShuaibi (2013)	M C Q F O	Total	10 sites in Kuwait City, Kuwait	03/2011–02/2012 (monthly)
Al-Dousari and Al-Awadhi (2012)	M + K + S C Q F O	Total	10 locations in Arabian Peninsula	11/2006–12/2007 (monthly)
Al-Dousari et al. (2013)	M + K + S C Q F O	Total	11 global locations	01/2007–12/2007 (monthly)
Arnold et al. (1998)	M K S Q F O	< 2 µm; 2–20 µm	1: North of Hawaii 2: Northeast Pacific	1: 05/1986 2: 03–04/1987
Aston et al. (1973)	1:M K S O; 2:C Q O	1:< 2 µm; 2: Total	Eastern North and South Atlantic, Indian Ocean, Sea of China	07/1971–11/1971
Avila et al. (1997)[a]	M K S C Q F O	Total	Montseny Mountains, Spain	11/1984–03/1992
Awadh (2012)	C Q F G O	Total	Baghdad, Iraq	03/2008–06/2008
Chester and Johnson (1971a)	M K S O	< 2 µm	Eastern Atlantic	11/06/1970–11/13/1970
Chester and Johnson (1971b)	M K S O	< 2 µm	Eastern Atlantic	04/22/1969–05/05/1969
Chester et al. (1971)	M K S O	< 2 µm	Eastern Atlantic	07/1970–08/1970
Chester et al. (1972)	M K S O	< 2 µm	Eastern Atlantic	03/17/1971–03/28/1971

Table 1. Continued.

Reference	Minerals	Size Range	Location	Time Range
Chester et al. (1977)	1:M K S O 2:Q C	1:$<2\,\mu$m 2: Total	Eastern Mediterranean	Summer 1972, Spring 1975
Chester et al. (1984)	M K S O	$<2\,\mu$m	Tyrrhenian Sea	10/08/1979–10/25/1979
Delany et al. (1967)	M K S Q O	$<2\,\mu$m	Barbados	10/1965–01/1966
Díaz-Hernández et al. (2011)	M K S C Q F G O	Total	Granada Depression, Spain	1992
Enete et al. (2012)	1:M K Q F 2:M K Q F I O	1:$<2\,\mu$m 2: 2–50 μm	2 sites in Enugu, Nigeria	10/2009–04/2010, 10/2010–04/2011 (weekly)
Engelbrecht et al. (2009)	M + K + S[b] C Q F I O	$<10\,\mu$m	14 site in Central and West Asia and 1 site in Djibouti	2005 to 2007
Engelbrecht et al. (2014)	M + K + S[b] C Q I[c] G O	$<2.5\,\mu$m	Las Palmas de Gran Canaria, Spain	01/12/2010–11/27/2010 (2 to 13 days)
Falkovich et al. (2001)	C Q F G	Total	Tel-Aviv, Israel	03/16/1998
Ferguson et al. (1970)	M K S O	$<2\,\mu$m	Northeasten Pacific	April 1969
Fiol et al. (2005)[d]	M K C Q F O	Total	Palma de Mallorca, Spain	05/06/1988–04/27/1999
Formenti et al. (2008)	M K C Q F[e]	$<40\,\mu$m	Banizoumbou, Niger	01/13/2006–02/13/2006
Game (1964)	C Q F I O	Total	East Atlantic	02/06/1962
Ganor (1991)	M K O	$<10\,\mu$m	Tel Aviv and Jerusalem, Israel	1968–1987
Ganor et al. (2000)	1:M K S O 2:C Q F	1: $<2\,\mu$m 2: $>=2\,\mu$m	16 locations around Lake Kinneret, Israel	01/1993–05/1997
Gaudichet et al. (1989)	M K S C Q F O	Total	Amsterdam Island, TAAF	05/15/1994–05/26/1984, 07/07/1984–07/30/1984, 09/05/1984–09/29/1984

Table 1. Continued.

Reference	Minerals	Size Range	Location	Time Range
Gaudichet et al. (1992)	M K S O	$< 2\,\mu\text{m}$	1: Vostok, 2: South Pole	1: 1927 2: 1955
Glaccum and Prospero (1980)	M K C Q F O	Total	Sal Island, Cape Verde; Barbados; Miami, Florida	07/1974–08/1974
Goldberg and Griffin (1970)	M K S O	$< 2\,\mu\text{m}$	1: Bay of Bengal 2: Waltair, India	1: 05/1968 2: 01/1969
Jeong (2008)	M K S C Q F O	$< 10\,\mu\text{m}$	Seoul, Korea	Spring 2003, 2004, 2005
Jeong and Achterberg (2014)	M + S K C Q F G O	$< 60\,\mu\text{m}$	1: Deokjeok Island, Korea 2: Andong, Korea 3: São Vicente, Cape Verde	1: 03/31/2012[f] 2: 03/16/2009–03/17/2009[f], 03/20/2010[f], 03/18/2014[f] 3: 12/28/2007–12/31/2007, 01/18/2008–01/23/2008
Jeong et al. (2014)	M + S K C Q F I G O	1: 5 size bins up to $60\,\mu\text{m}$ 2: $< 60\,\mu\text{m}$	1: Deokjeok Island, Korea 2: Andong, Korea	1: 03/31/2012–04/01/2012[f] 2: 03/20/2010[f], 05/01/2011[f]
Johnson (1976)	1: M S O 2: M + K + S[g] Q F	1: $< 2\,\mu\text{m}$ 2: Total	3 in Atlantic; Barbados	12/1898; 10/1965; 03/1971
Kandler et al. (2007)	M C Q F I G O	8 size bins 0.05 to $20\,\mu\text{m}$[h]	Izaña, Tenerife, Canary Islands, Spain	07/13/2005–07/23/2005, 08/06/2005–08/08/2005
Kandler et al. (2009)	M K C Q F I G O	10 size bins 0.1 to $250\,\mu\text{m}$[i]	Tinfou, Morocco	05/13/2006–06/07/2006

Table 1. Continued.

Reference	Minerals	Size Range	Location	Time Range
Kandler et al. (2011)	M[j] K S C Q F G O	Total	Praia, Cap Verde	01/14/2008–02/09/2008 (daily)
Khalaf et al. (1985)	M + S K C Q F G O	<4 µm	8 location in Kuwait	04/1979–03/1980
Leinen et al. (1994)	M K S Q F O	1: <2 µm; 2: 2–20 µm	Northwest and East Pacific	09/1977–10/1979
Lu et al. (2006)	M K S Q F O	<10 µm	Beijing, China	04/2002–03/2003
Menéndez et al. (2007)	M K[k] C Q F O	Total	Gran Canaria, Canary Islands, Spain	10/31/2002–10/23/2003
Møberg et al. (1991)	M K S Q F I O[l]	<2 µm	Zaria, Nigeria	11/1984–03/1985
O‘Hara et al. (2006)	M K C Q F G O	Total	1: Northern Libya 2: Southern Libya	06/2000–05/2001
Parkin et al. (1970)	M S Q O	Total	North Atlantic	01/1969 and 08/1969
Parkin et al. (1972)	M S Q O	Total	Central Atlantic	02/1971–03/1971
Prospero and Bonatti (1969)	M K S Q F O	<20 µm	East Pacific	Spring 1967
Prospero et al. (1981)	M K Q F C I G O	Total	1: Cayenne 2: Dakar, Barbados, Cayenne	1: 12/1977–04/1980 2: 03/21/1978–03/27/1978
Queralt-Mitjans et al. (1993)	M K C Q F G O	Total	7 locations at Filabres Range, Spain	11/1989–12/1989, 03/1990–05/1990
Rashki et al. (2013)	M C Q F G O	<75 µm	2 locations in Sistan Region, Iran	08/2009–08/2010
Shao et al. (2008)	1: M K S[m] O 2: M + K + S C Q F G O	1: <2 µm 2: Total	Beijing, China	1 + 2: 04/17/2006, Spring 2006 2: Spring 2004, 2005
Shen et al. (2006)	M K C Q F O	Total	Dunhuang, China	Spring 2001 and 2002
Shen et al. (2009)	M C Q F O	Total	5 locations in desert regions of China	Spring 2001 and 2002

Table 1. Continued.

Reference	Minerals	Size Range	Location	Time Range
Shi et al. (2005)	1: M K S O 2: M + K + S C Q F I G 3: M + K + S C Q F O	1: $< 2\,\mu$m 2: $< 10\,\mu$m 3: Total	Beijing, China	04/06/2000 and 03/20/2002 (1 and 2 only)
Skonieczny et al. (2013)	M K S O[n]	$< 30\,\mu$m	Mbour, Senegal	02/23/2006–03/27/2009 (weekly)
Tomadin et al. (1984)	M K S O	$< 2\,\mu$m	1: Central ~~Mediterrenean~~Mediterranean 2: Central ~~Mediterrenean~~Mediterranean 3: Scilla, Messina, Bologna	1: 03/1981 2: 10/1981–11/1981 3: 03/1981
Windom (1969)	M K S Q F O	Total	5 permanent snow fields on planet	before 1969
Zdanowicz et al. (2006)	M K S O	Total	St. Elias Mountains, Canada	04/16/2001
Zhou and Tazaki (1996)	I + K + S C Q G O	Total	Matsue, Japan	10/1992–09/1993 (weekly)

[a] only Red Rain events;
[b] may contain chlorite;
[c] may contain rutile or pyrolusite;
[d] only Red Rain events;
[e] all minerals: percentage of refractive surface (XRD);
[f] dust event;
[g] includes chlorite;
[h] used here: 1–2.5, 2.5–5, 5–10, and 10–20 µm ranges;
[i] interpolated to ModelE2 size bins;
[j] as part of mixed layer illite-smectite;
[k] kaolinite-chlorite;
[l] all minerals: from maximum and minimum value;
[m] as part of mixed-layer illite-smectite;
[n] mineralogy of aluminosilicates only.

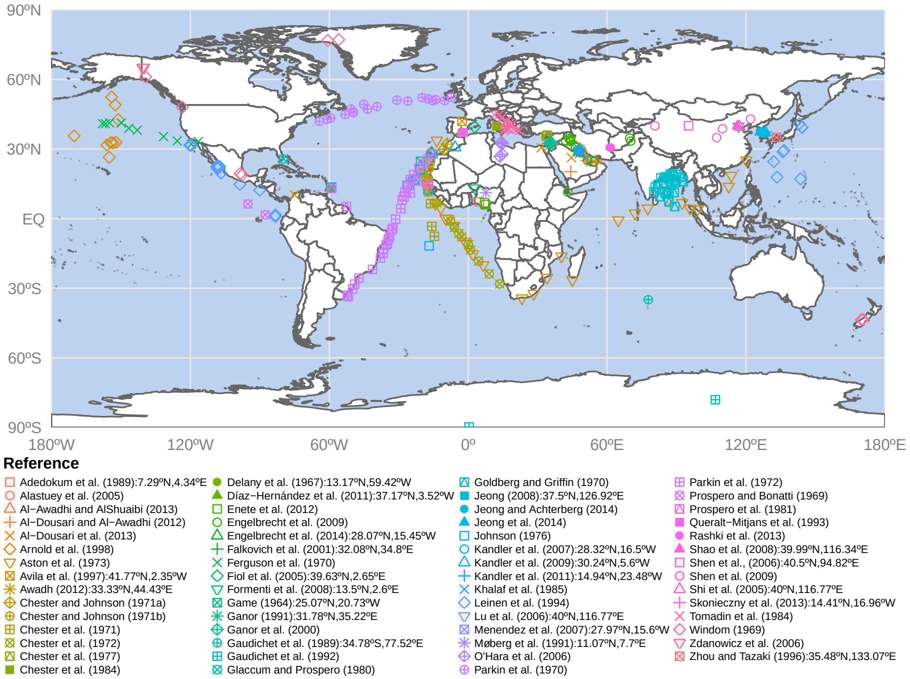

Figure 1. Locations of measured mineral fractions compiled from the literature used for the evaluation of the simulations. References with geographical coordinates in the legend provide measurements only for this single location; otherwise, references provide measurements for multiple locations. See Table 1 and Table S1 in the Supplement for more information.

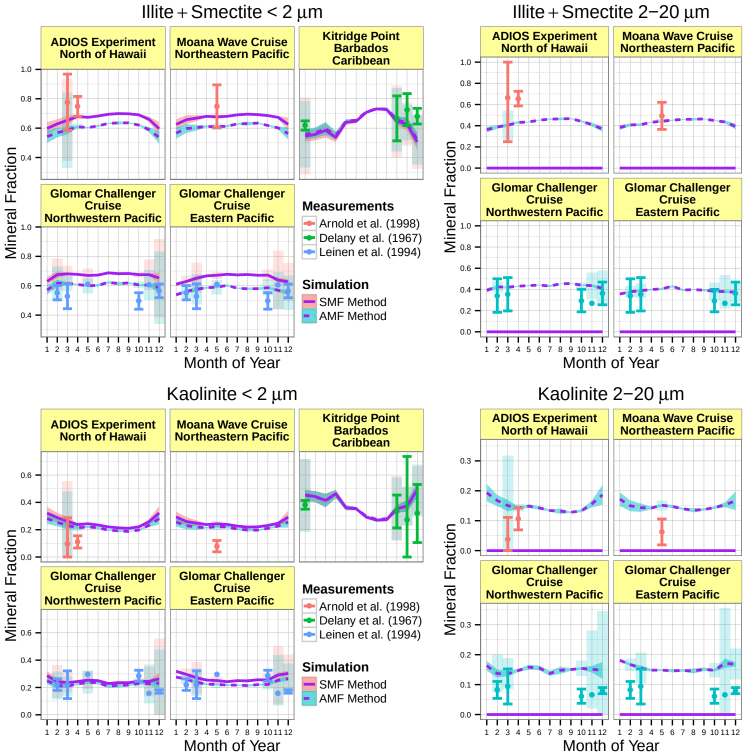

Figure 2. Annual cycle of illite plus smectite and kaolinite fractions for diameters less than 2 µm and from 2 to 20 µm as measured and simulated by the SMF and AMF methods. The vertical error bars, shaded ribbons, and shaded bars represent the 95 % confidence intervals of the measurements, the simulations (based on monthly SDs), and the simulations sampled at the frequency of the measurements, respectively.

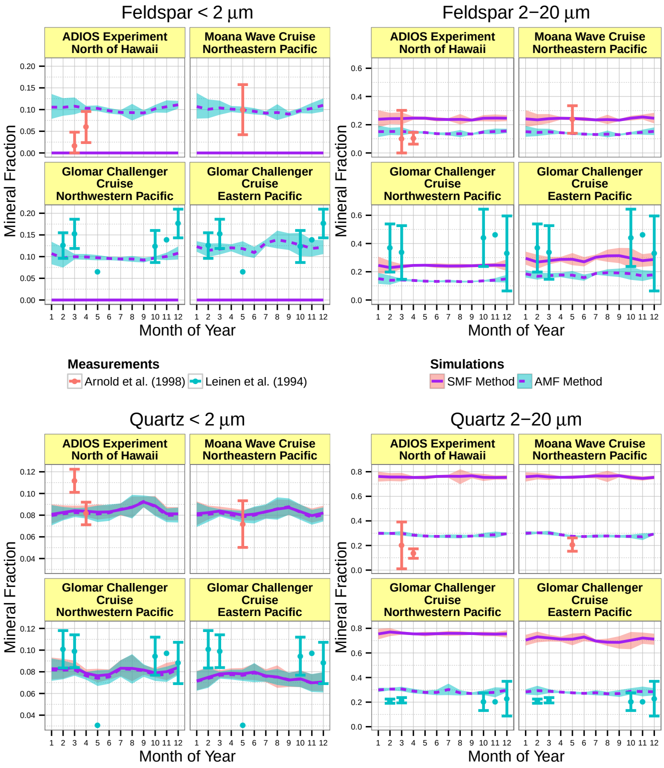

Figure 3. Same as Fig. 2 but for feldspar and quartz.

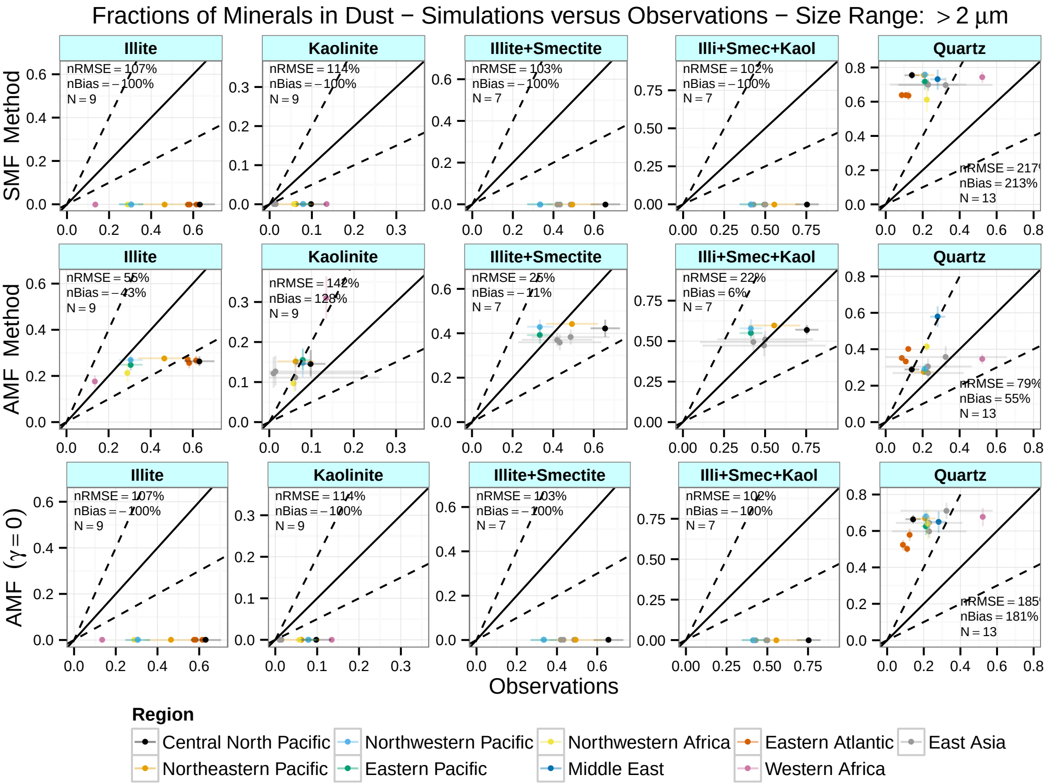

Figure 4. Scatter plot of mineral fractions of illite, kaolinite, the sum of illite and smectite, all phyllosilicates and quartz for silt particles (whose diameters are greater than 2 µm) simulated by the SMF, AMF and AMF ($\gamma = 0$) experiments vs. measurements. The dashed lines mark ratios of 2 : 1 and 1 : 2 between the simulated and observed mineral fractions. The horizontal and vertical error bars show the 95 % confidence ~~intervals~~interval.

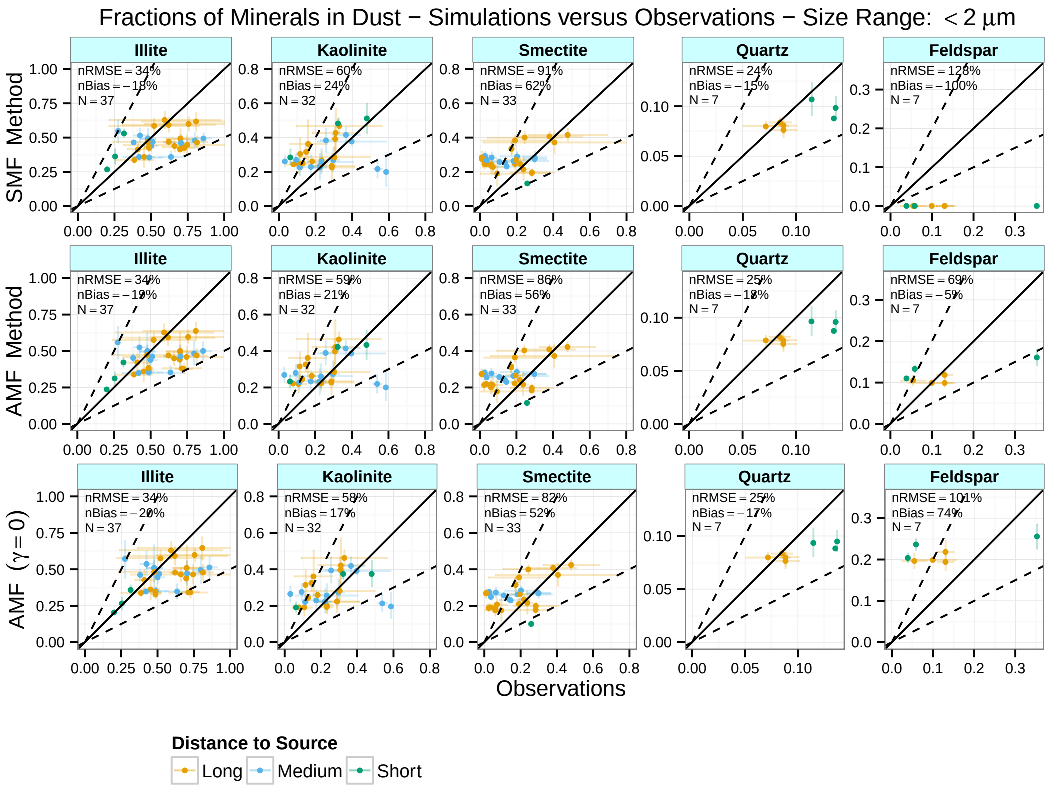

Figure 5. Same as Fig. 4 but for illite, kaolinite, smectite, quartz, and feldspar at clay diameters (less than 2 µm).

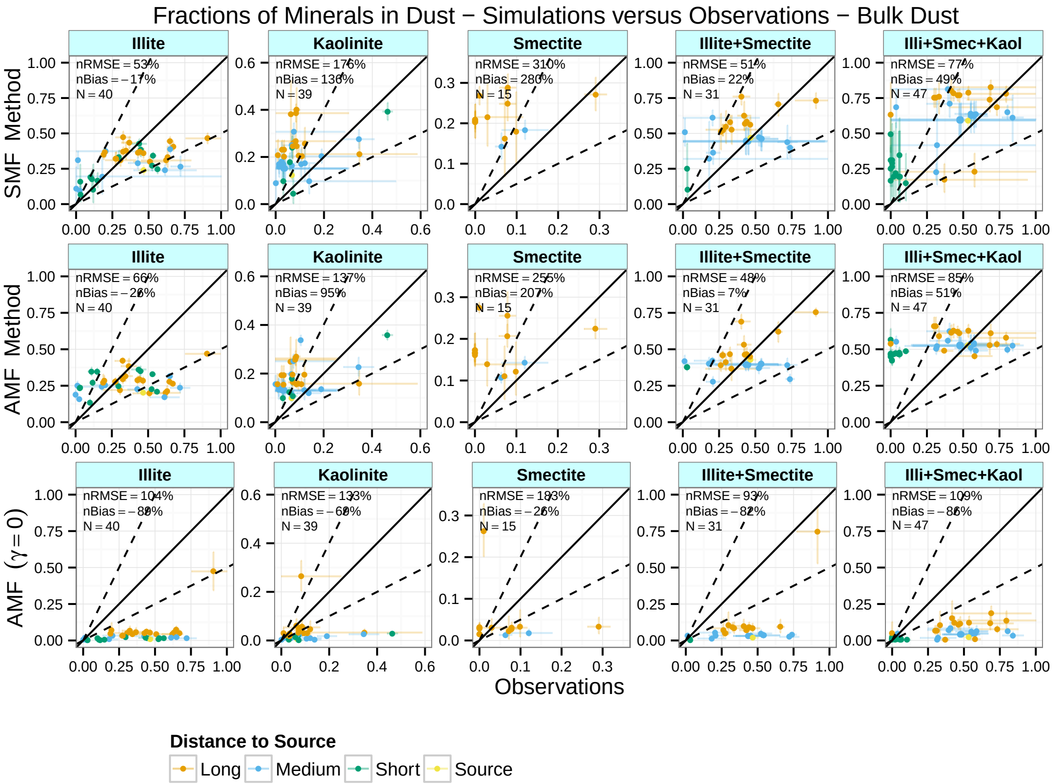

Figure 6. Same as Fig. 4 but for bulk (clay plus silt) mineral fractions of illite, kaolinite, smectite, the sum of illite and smectite, and all phyllosilicates.

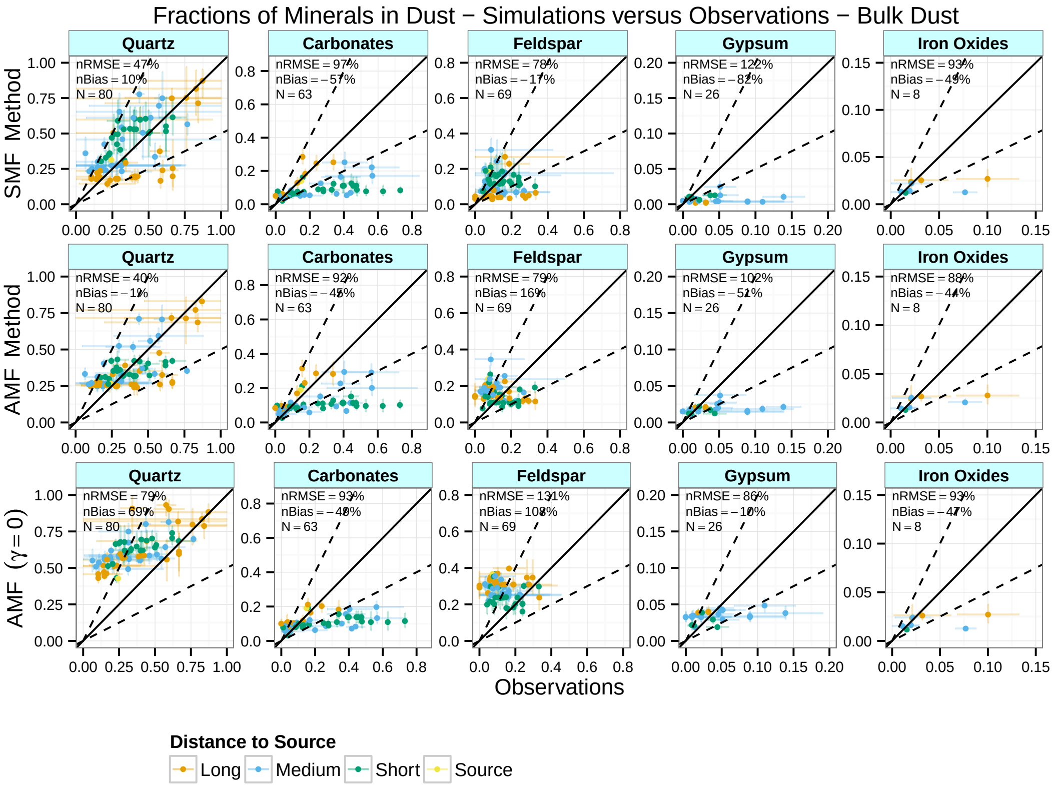

Figure 7. Same as Fig. 4, but for bulk mineral fractions of quartz, carbonates, feldspar, gypsum, and iron oxides.

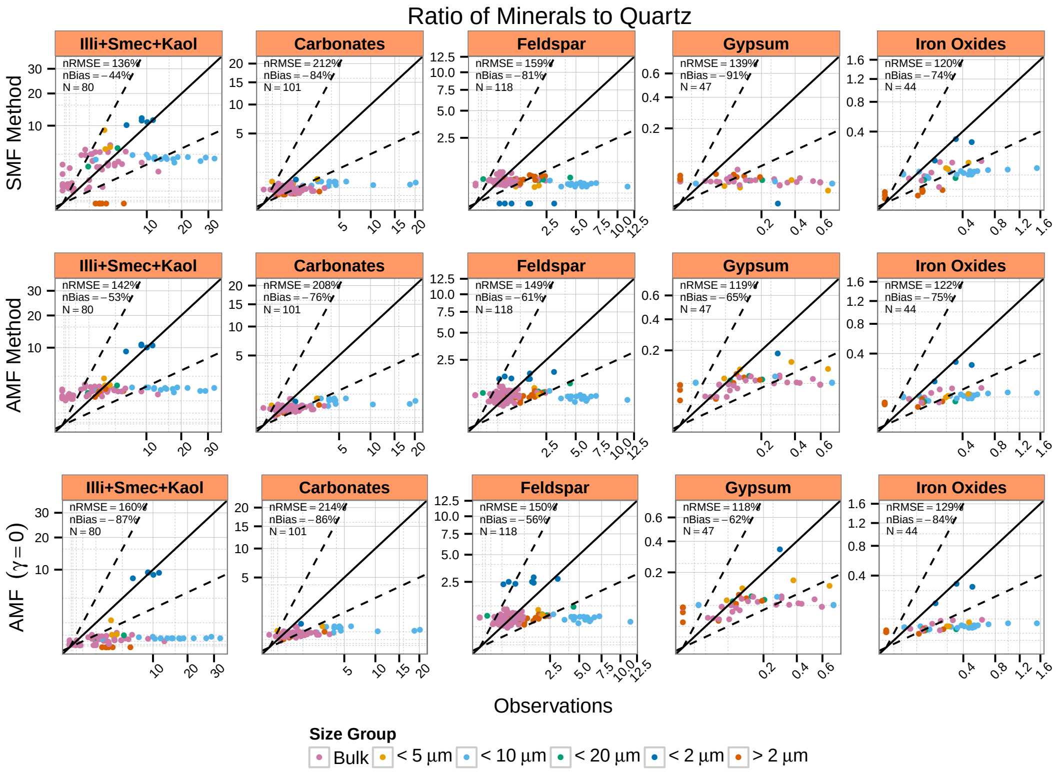

Figure 8. ~~Figure 9.~~ Measured vs. simulated mineral ratios with respect to quartz for the SMF, AMF and AMF ($\gamma = 0$) methods. The dashed lines mark a ratio of $2:1$ and $1:2$ between the simulated and observed mineral ratios.

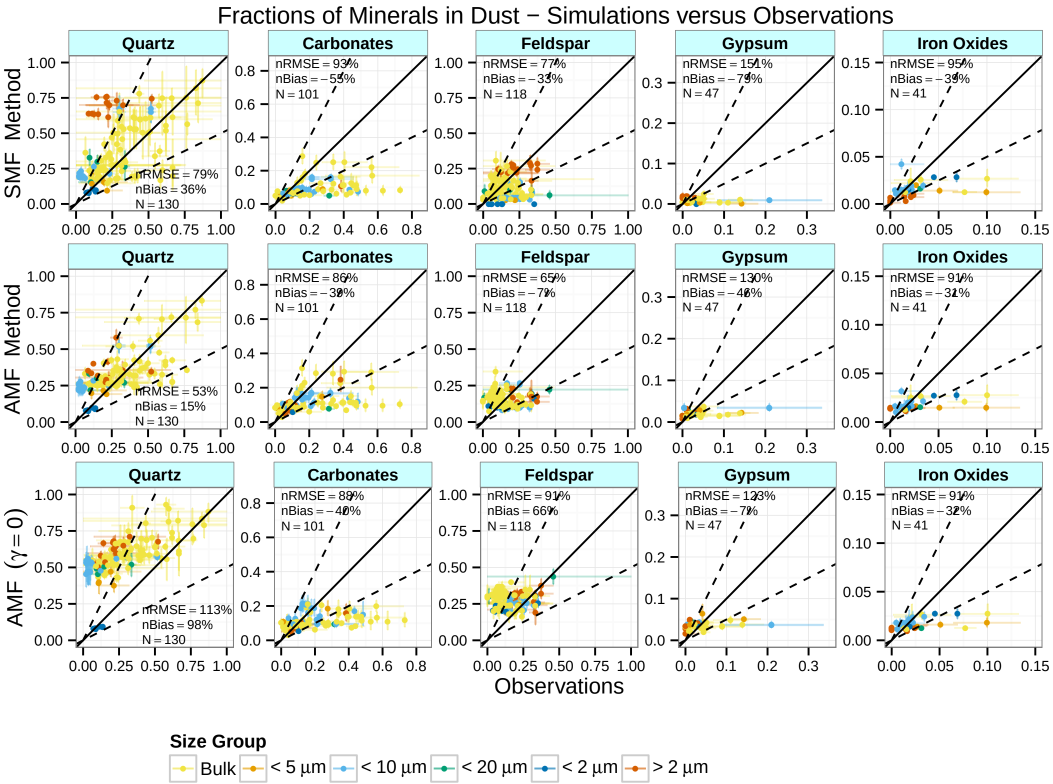

Figure 9. ~~Figure 8.~~ Same as Fig. 4, but including particle mass (PM) measurements at other size ranges.